Preparation and Characterization of Novel Montmorillonite Nanocomposites

Rola Mansa

Thesis submitted to the
Faculty of Graduate and Postdoctoral Studies
in partial fulfillment of the requirements
For the MSc degree in Chemistry

Department of Chemistry
Faculty of Science
University of Ottawa

Acknowledgments

I would like to express my deepest gratitude to my research supervisor, Professor Christian Detellier, who has been an unlimited source of guidance and an excellent mentor to me throughout this project. His outstanding knowledge and incomparable professionalism and enthusiasm for the subject matter have truly made my studies an enjoyable, informative and memorable experience.

My heartfelt appreciation goes to my family for their continuous support. I would especially like to thank my mother for her inexhaustible encouragement, support and love.

I would like to thank the members of the Detellier research group as well as Professors Claude Forano and Vanessa Prévot for their discussions and insight.

I would also like to thank the members of my committee for taking the time to examine my thesis and partake in my defence.

For my late father, Hanna Manassa, who nurtured determination and confidence in me and always cherished an ambitious image for me. His love and support was, and always will be, priceless to me.

Abstract

Clay minerals have historically played a consequential role in human health. While the beginnings were rooted in geophagy, a primitive act of consuming earth, the health-related uses of clay minerals have evolved and diversified over time.

As excipients in pharmaceutical formulations, clay minerals can attribute novel properties onto intercalated compounds. Intercalating oxybenzone, a UV filter, within the interlamellar space of montmorillonite is desirable in order to minimize direct contact with skin. Intercalating resveratrol, a compound known for attributing beneficial effects onto human health, may be advantageous since this compound is susceptible to cis-trans isomerisation. The strategy of using alkylammonium–modified clay was undertaken and proved successful for the intercalation of oxybenzone.

The field of biopolymer/layered silicate nanocomposites is heavily researched for use in a multitude of applications. Novel montmorillonite nanocomposites were prepared with neutral guar gum and cationic guar gum, using an environmentally friendly process and are fully characterized.

Table of Content

List of Tables and Figures

Abbreviations

SWy-2	Montmorillonite from Wyoming, USA
Na^+ MMT	Sodium saturated montmorillonite
CEC	Cation exchange capacity
d_{001}	Basal spacing
CTAB	Cetyltrimethylammonium bromide
CTA	Cetyltrimethylammonium ion
CTA-MMT	Montmorillonite modified with cetyltrimethylammonium ions
OXY + CTA-MMT	Cetyltrimethylammonium-montmorillonite modified with oxybenzone.
RESV + CTA-MMT	Cetyltrimethylammonium-montmorillonite modified with resveratrol (attempt).
CTA-MMT BLANK	A blank experiment performed where cetyltrimethylammonium-montmorillonite was dispersed in methanol, with the absence of adsorbate.
CG	Cationic guar gum
NG	Neutral guar gum
CG-MMT 3:1	Cationic guar-montmorillonite nanocomposite prepared using a 3:1 ratio of cationic guar to montmorillonite.
NG-MMT 3:1	Neutral guar-montmorillonite nanocomposite prepared using a 3:1 ratio of neutral guar to montmorillonite.
NG-MMT 6:1	Neutral guar-montmorillonite nanocomposite prepared using a 6:1 ratio of neutral guar to montmorillonite.
NG BLANK	A blank experiment performed where neutral guar gum was dispersed in water, with the absence of montmorillonite.
XRD	X-ray diffraction

TGA	Thermogravimetric analysis
NMR	Nuclear magnetic resonance
TEM	Transmission electron microscopy
MAS	Magic angle spinning
CP	Cross polarization

CHAPTER 1

Introduction

1.1 The chemistry of clay minerals

Clay minerals are hydrous layered silicates belonging to the family of phyllosilicates (Bailey, 1980). They compose the colloid fraction, with a particle size less than 2 μm, of soils and sediments (Pinnavaia, 1983). The configuration of clay minerals can be defined in terms of layers and sheets. The basic structural unit of clay minerals is the sheet structure which consists of oxygen coordinated to various cations such as Al^{3+} and Si^{4+} (Kloprogge *et al.*, 1999). An assemblage of sheets constitutes a layer. The sheets are arranged in different sequences to form different clay minerals. A cation coordinated to four oxygen atoms forming a tetrahedron is linked to adjacent tetrahedra through the sharing of three oxygen atoms and this linkage constitutes the tetrahedral sheet (Brigatti *et al.*, 2006; Bailey, 1980). The common cations of the tetrahedral sheet are Si^{4+}, Al^{3+}, and Fe^{3+} (Brigatti *et al.*, 2006). The tetrahedral units are arranged in the form of a hexagonal network. The apical oxygen of the tetrahedral unit connects to the adjacent octahedral sheet (Bailey, 1980; Kloprogge *et al.*, 1999). Edge-shared octahedral coordinated by oxygen and hydroxyls with Al^{3+}, Fe^{3+}, Mg^{2+} and Fe^{2+} as the common cations, constitute the octahedral sheet (Brigatti *et al.*, 2006).

Variations in the properties of the clay minerals are explained by the structural and chemical characteristics of the layers. The composition of the layers offers a convenient classification system (Bailey, 1980; Martin *et al.*, 1991). The linkage of one tetrahedral sheet with one octahedral sheet forms the 1:1 layer, commonly known as the TO layer

(Fig. 1). The sandwiching of an octahedral sheet between two tetrahedral sheets forms the 2:1 layer structure, also known as the TOT layer (Fig. 2). The layers are continuous in the *a* and *b* directions and are stacked atop each other in the *c* direction (Bhattacharya & Gupta, 2008).

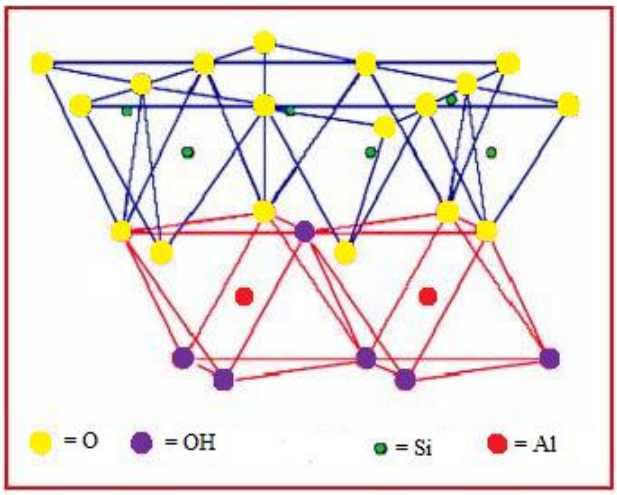

Figure 1. Structure of kaolinite, a 1:1 layered clay mineral (Adapted from Bhattacharya & Gupta, 2008).

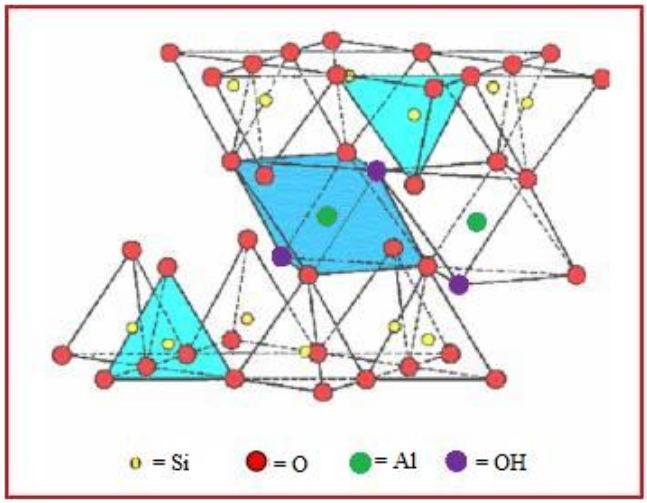

Figure 2. Structure of montmorillonite, a 2:1 layered clay mineral (Adapted from Bhattacharya & Gupta, 2008).

1.2 Structural features of montmorillonite

Smectites are one of the largest classes of clay minerals (Kloprogge *et al.*, 1999), with montmorillonite, a member of the smectite family, as the most important in the industrial field (Murray, 2000). Two tetrahedral sheets sandwich an octahedral sheet to form a montmorillonite layer, classifying montmorillonite as a 2:1 clay mineral. In comparison to other minerals with a 2:1 layered structure, such as talc and pyrophyllite, montmorillonite exhibits isomorphic substitution (Yariv and Michaelian, 2002). The substitution of Si^{4+} by Al^{3+} in the tetrahedral sheet and Al^{3+} by Mg^{2+} in the octahedral sheet causes a charge deficiency, which is counterbalanced by exchangeable cations including K^{+}, Na^{+}, Ca^{2+} and Mg^{2+}, located between the parallel clay layers and around the edges of the layers (Murray, 2000; Brigatti *et al*., 2006). The negative charge of the layers can be quantified as the cation exchange capacity (CEC) which is the propensity that smectites have for absorbing cationic species from solution (Brigatti *et al*., 2006). The interlamellar cations of montmorillonite are hydrated, rendering montmorillonite a swelling clay. Upon swelling, water enters the interlayer space causing an expansion in the *c* direction (Bhattacharya & Gupta, 2008). Intercalation by organic cations, through cationic exchange with the interlamellar inorganic cations, also causes an expansion in the c-direction, which can be monitored by X-ray diffraction. Organophilicity is consequently attributed to the clay surface, enhancing its compatibility with other organic compounds (Bhattacharya & Gupta, 2008; Ganguly *et al.*, 2010).

1.3 Therapeutic applications of clay minerals

The applications of clay for therapeutic purposes have existed since as far back as the dawn of mankind (Gomes & Silva, 2007). Geophagy, the deliberate consumption of earth, was presumably practiced by Homo erectus and Homo neanderthalensis (Ferrell, 2008; Klein *et al.*, 2008). As researched by Bech (1987), Robertson (1996), and Veniale (1997), and cited by Carretero (2002), in ancient Egypt and Mesopotamia, clay was used as an anti-inflammatory agent. Hippocrates and Aristotle attested to the value of clays during the ancient Greek period by creating classifications of medicinal earths, most of which were clays. During that time period, mud was used as an antiseptic cataplasm, cicatriser and as a cure for snake bites, as researched by Bech (1996) and Giammatteo *et al.* (1997) and cited by Carretero (2002). As researched by Bech (1987), and Veniale *et al.* (1999), and cited by Carretero (2002), during the 9^{th} and 10^{th} centuries, the use of clays for the treatment of malaria was encouraged.

Clays are nowadays widely used in conventional pharmaceutical applications as excipients and active agents. As excipients, the inertness of clay minerals, along with their structural and physicochemical properties, are exploited to perform a technological function. Smectites can fulfill the role of an excipient through use as a disintegrant, where the ability to take up water or to disperse in water favours the liberation of an active ingredient in a pharmaceutical formulation (Carretero, 2002). A range of minerals, that include both kaolinites and smectites, are used as diluents of the concentration of organic ingredients, and this facilitates the administration of a drug at a certain dose; in this case, the inherent inertness of clay minerals is advantageous. Moreover, the facilitation of the compaction of

tablets and granules, through the use of clay minerals as a binder, is also widely acknowledged (Carretero & Pozo, 2009). Palygorskite and smectites are often used as emulsifiers and thickeners in formulations due to their colloidal properties (Carretero & Pozo, 2009; Carretero, 2002).

Of specific interest is the excipient role that clay minerals play as carriers of active compounds. The characteristic of a large specific surface area and a high adsorption capacity makes clay minerals advantageous for such a purpose (Carretero, 2002). In particular, the novel physical and chemical properties acquired by the intercalation of the active compound within the clay layers, has led to the development and investigation of various organic-clay hybrids. For example, the intercalation of 5-fluorouracil into montmorillonite for use as a sustained release carrier was performed by Lin *et al.* (2002). 5-fluorouracil is the only effective chemotherapy option for colorectal cancer and its use is associated with an incomplete and unpredictable absorption when administered orally, due to its degradation in the gastrointestinal tract. The intercalation was performed in the goal of designing a 5-fluorouracil carrier system capable of releasing the active compound in-situ of the cancer area (Lin *et al.*, 2002).

As active agents, clay minerals perform particular therapeutic functions when applied topically or ingested. In this case, the physical properties and the chemical composition of the clay minerals determine the therapeutic uses, with the main uses being treatments of gastrointestinal or skin disorders (Carretero & Pozo, 2010; Viseras *et al.*, 2010). For example, the high sorption capacity and large specific surface area of some clay minerals, such as palygorskite, sepiolite, kaolinite and smectite, provides them with the ability to adhere to the gastric and intestinal mucous membrane, and uptake gases, toxins, bacteria and

viruses. The ability of smectites to adsorb protons attests to their ability to function as an antiacid. In fact, the properties of smectites, which include their high sorption and swelling capacities, as well as cation exchange capabilities, allow for several applications in the pharmaceutical industry (Carretero & Pozo, 2010; Droy-Lefaiz & Tateo, 2006).

Topically applied clay minerals serve particular functions as active agents. In this capacity, clay minerals can be used as dermatological protectors. Once applied, the clay minerals can adhere to the skin and adsorb undesirable skin exudations through the characteristics of high sorption capacity and large surface area. Moreover, the minerals can form a film onto the skin, thereby providing a mechanical barrier against external, physical and chemical stress and serve as dermatological protectors (Carretero, 2002). Applied as a poultice, the heat retention properties of kaolinite serve to relieve pain associated with inflammation (Carretero & Pozo, 2010). Moreover, clay minerals are also used in spas and in aesthetic medicine. The process of geotherapy, whereby a mixture of clay and water is applied to the afflicted area, is used to treat dermatological afflictions. During pelotherapy, clay is made to undergo maturation and is applied topically for the resultant stimulatory, antiphlogistic, and analgesic action, and also for the treatment of dermatological afflictions. Paramuds, which are mixtures of paraffin and mud, are applied for the purpose of moisturizing the skin (Carretero, 2002).

1.4 Objectives

An important aspect of dermatological protection involves the application of sunscreen. This is propelled by the well known fact that exposure to UV rays results in adverse reactions, those of which include short-term inflammatory responses (erythema and sunburn) and long-term effects (cutaneous photoageing, immunosuppression and skin cancers) (Cals-Grierson & Ormerod, 2004; National Institute of Health, 1989; Yaar & Gilchrest, 2007; Ziegler *et al.*, 1994). Sunscreen is used to decrease the amount of solar radiation reaching the skin by the absorption of UV rays, preventing radiation transfer onto the skin (Touitou & Godin, 2008; Perugini *et al.*, 2002). However, the photoinstability of certain UV filters is a major concern due to a diminishment of their UV protective capacities (Lowe, 2006; Perioli *et al.*, 2006; Perugini *et al.*, 2002).

Furthermore, the potential for phototoxic or photoallergic contact dermatitis, as caused by the reactive intermediates of photounstable UV filters, necessitates the development of strategies for improving conventional sunscreen formulations (Gaspar & Campos, 2006; Deflandre & Lang, 1988; Antoniou *et al.*, 2008; Perioli *et al.*, 2006). A new strategy is being researched as of late, which involves providing a protective barrier around the UV absorbing agent, for example, by complexation with cyclodextrin (Scalia *et al.*, 2004), or by intercalating into layered double hydroxides (Perioli *et al.*, 2006), or zeolites (Chrétien *et al*, 2010).

Oxybenzone (Fig. 3), 2-hydroxy-4-methoxybenzophenone, is a frequently used UV filter (Antoniou *et al.*, 2008; Schallreuter *et al.*, 1996). Its use is associated with reported incidences of photoallergy (Langan & Collins, 2006; Silva *et al.*, 1995; Zhang *et al.*, 1998;

Collins & Ferguson, 1994). In addition, oxybenzone is found to penetrate the epidermal barrier via topical applications and is excreted in urine, according to a study performed. The amount adsorbed is estimated to be up to 1–2% of the applied amount (Hayden *et al.*, 1997).

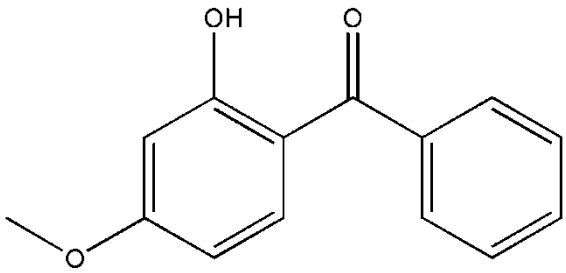

Figure 3. Structure of oxybenzone.

To thwart the adverse reactions associated with the topical application of oxybenzone, preventing direct contact of the UV filter with the skin by using a lamellar host is an attractive strategy (Perioli *et al.*, 2006). Intercalation of oxybenzone within the clay mineral montmorillonite is advantageous for a variety of reasons. Clay minerals are the most abundant minerals on the planet (Vorhies & Gaines, 2009). Clay minerals have been used for their curative properties for thousands of years and are currently already widely used in the pharmaceutical industry as both excipients and active agents, as well as in the cosmetic industry. The lack of toxicity of montmorillonite, compounded by its chemical inertness, attests to its suitability for use in close contact with skin (Carretero, 2002).

Resveratrol (3,4',5-trihydroxy-trans-stilbene) (Fig. 4) is another interesting compound that may benefit from being incorporated into a suitable drug carrier, such as montmorillonite. This phenolic compound is naturally found in many plant sources; its production by plants is a reaction to exogenous stress factors (Shi *et al.*, 2008). Resveratrol

is found in foods such as grapes, red wine, and cocoa (Counet *et al.*, 2006; Gao *et al.*, 2002). Interestingly, a rich source of resveratrol is found in the roots of *Polygonum Cuspidatum*, a prominent plant in traditional Chinese medicine that is used to combat ailments such as inflammation, allergy, etc. (Shi *et al.*, 2008; Vastano *et al.*, 2000). It is well known that resveratrol imparts a multitude of beneficial effects onto human health including antioxidative effects (Pandey & Rizvi, 2010), anti-inflammatory effects (Ølholm *et al.*, 2010), and most notably, anticancer effects (Jang *et al.*, 1997). However, it was observed that in solution, more than 80% of the trans-resveratrol isomerized to cis-resveratrol after being exposed to daylight for 1 hour (Vian *et al.*, 2005). As mentioned previously, clay minerals are an excellent choice for the purpose of intercalating active compounds for a variety of reasons, including the lack of toxicity, high sorptive capacity and natural abundance. Intercalating resveratrol within a clay nanocomposite may be advantageous since intercalation is usually associated with improved stability and other properties advantageous for pharmaceutical purposes (Dornelas *et al.*, 2011).

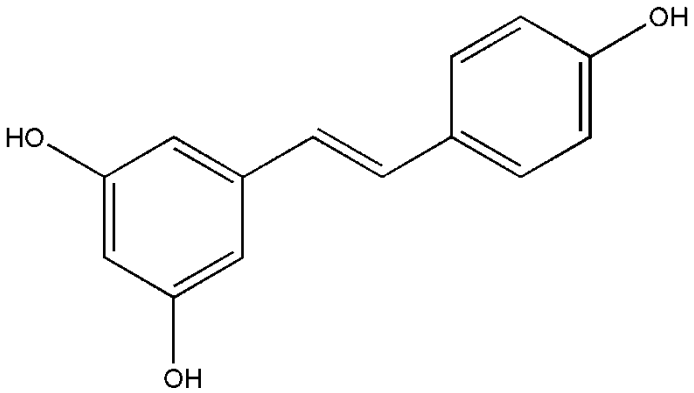

Figure 4. Structure of resveratrol.

The emerging field of polymer clay nanocomposites represents another important facet of the pharmaceutical applications of clay minerals (Viseras *et al.*, 2007). Polymer

nanocomposites can be generally defined as the combination of polymer and organic filler at the nanometer scale (Hule & Pochan, 2007). These materials are highly versatile and interdisciplinary (Wu *et al.*, 2010), finding applications in many avenues of academia and industry. Their versatility is owed to the assortment of polymers and fillers obtainable by researchers. A distinctive property of polymer nanocomposites is their improved mechanical properties, which stems from the nanometer scale interaction between the filler and the polymer (Hule & Pochan, 2007). Layered clays are commonly used as fillers and the resultant polymer-clay nanocomposites have garnered significant attention due to a notable acquisition of enhanced chemical and/or mechanical properties (Krikorian & Pochan, 2003). The lamellar design of clay minerals, compounded with their high aspect ratio and large surface area, are attractive for the design of polymer nanocomposites as drug vehicles (Gupta & Bhattacharya, 2008). The synergism of characteristics belonging to the parent constituents results in the formation of materials exhibiting properties ideal for pharmaceutical use including improved stability, compactability and solubility (Dornelas *et al.*, 2011). Compounded with the intercalation capacity of clay minerals, polymer-clay nanocomposites possess the potential for use as controlled release systems (Suresh *et al.*, 2010). In particular, montmorillonite is a main choice due to its low cost and its rich intercalation chemistry, which is attributed to its exchangeable interlamellar cations. Exchange of the interlamellar cations with other organic cations can circumvent incompatibility issues between polymer and filler (Gupta & Bhattacharya, 2008; Patel *et al.*, 2006).

This work is ultimately an investigation of the chemistry of the clay mineral montmorillonite, from a pharmaceutically-interesting perspective, with a two-fold objective:

- To intercalate resveratrol and oxybenzone, which are compounds of pharmaceutical interest, into montmorillonite.
- To develop novel nanocomposites based on montmorillonite and guar gum.

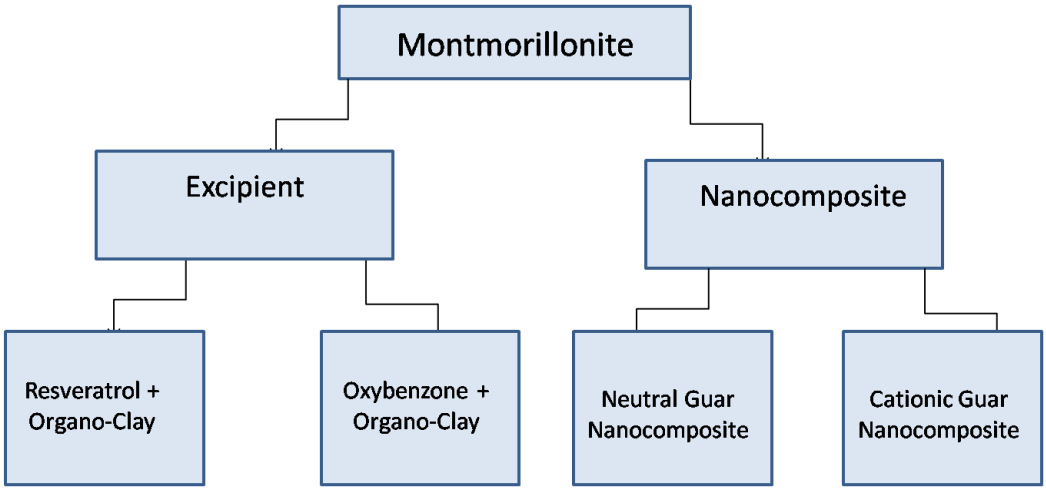

Figure 5. Illustration of the organization of the thesis.

References

Antoniou, C., Kosmadaki, M. G., Stratigos, A. J., & Katsambas, A. D. (2008). Sunscreens-what's important to know. *Journal of the European Academy of Dermatology and Venereology*, *22*(9), 1110-1119.

Bech, J. (1987). *Les Terres Medicinales*. Discurs per Reial Academia de Farmácia de Barcelona. Ed. Reial Academia de Farmácia de Barcelona-CIRIT (Generalitat de Catalunya), Barcelona, 105 pp.

Bech, J. (1996). Aspectos históricos y técnicos de las arcillas de uso medicinal. In: *IX Simp. Grupo Especializado de Cristalografia. La Cristalografia y la Industria* Farmacéutica. Ed. Reales Soc. Esp. Fısica y Quımica. Univ. Granada, pp. 15 – 17.

Bhattacharya, K. G., & Gupta, S. S. (2008). Adsorption of a few heavy metals on natural and modified kaolinite and montmorillonite: A review. *Advances in Colloid and Interface Science, 140*(2), 114-131.

Brigatti, M. F., Galan, E., & Theng, B. K. G. (2006). Structures and mineralogy of clay minerals. In F. Bergaya, B. K. G. Theng & G. Lagaly (Eds.), *Handbook of Clay Science* (pp. 19-85). Amsterdam: Elsevier Science.

Bailey, S. W. (1980). Structures of layer silicates. In G. W. Brindley & G. Brown (Eds.), *Crystal structures of clay minerals and their X-ray identification* (pp. 1-124). London: Mineralogical Society.

Cals-Grierson, M., & Omerod, A. D. (2004). Nitric oxide function in the skin. *Nitric Oxide, 10*(4), 170-193.

Carretero, M. I., & Pozo, M. (2009). Clay and non-clay minerals in the pharmaceutical

industry: Part I. Excipients and medical applications. *Applied Clay Science, 46*(1), 73-80.

Carretero, M. I. (2002). Clay minerals and their beneficial effects upon human health. A review. *Applied Clay Science, 21*(3-4), 155-163.

Carretero, M. I., & Pozo. (2010). Clay and non-clay minerals in the pharmaceutical and cosmetic industries: Part II. Active Ingredients. *Applied Clay Science, 47*(3-4), 171-181.

Chrétien, M. N., Heafey, E., & Scaiano, J. C. (2010). Reducing adverse effects from UV sunscreens by zeolite encapsulation: Comparison of oxybenzone in solution and in zeolites. *Photochemistry and Photobiology, 86*(1), 153-161.

Collins, P., & Ferguson, J. (1994). Photoallergic contact dermatitis to oxybenzone. *British Journal of Dermatology, 131*(1), 124-129.

Counet, C., Callemien, D., & Collin, S. (2006). Chocolate and cocoa: New sources of trans-resveratrol and trans-piceid. *Food Chemistry, 98*(4), 649-657.

Deflandre, A., & Lang, G. (1988). Photostability assessment of sunscreens. Benzylidene camphor and dibenzoylmethane derivatives. *International Journal of Cosmetic Science, 10*(2), 53-62.

Dornelas, C. B., Silva, A. M., Dantas, C. B., Rodrigues, C. R., Coutinho, S. S., Sathler, P. C., Castro, H. C., Dias, L. R. S., Sousa, V. P., & Cabral, L. M. (2011). Preparation and evaluation of a new nano pharmaceutical excipients and drug delivery system based on polyvinylpyrrolidone and silicate. *Journal of Pharmacy & Pharmaceutical Sciences, 14*(1), 17-35.

Droy-Lefaiz, M. T., & Tateo, F. (2006). Clays and clay minerals as drugs. In F. Bergaya, B.

K. G. Theng & G. Lagaly (Eds.), *Handbook of Clay Science* (pp. 743-752). Amsterdam: Elsevier.

Ferrell, R. E. (2008). Medicinal clay and spiritual healing. *Clays and Clay Minerals, 56*(6), 751-760.

Ganguly, S., Dana, K., & Ghatak, S. (2010). Thermogravimetric study of n-alkylammonium-intercalated montmorillonites of different cation exchange capacity. *Journal of Thermal Analysis and Calorimetry, 100*(1), 71-78.

Gao, L., Chu, Q., Ye, J. (2002). Determination of trans-resveratrol in wines, herbs and health food by capillary electrophoresis with electrochemical detection. *Food Chemistry, 78*(2), 255-260.

Gaspar, L. R., & Campos, P. M. B. G. (2006). Evaluation of the photostability of different UV filter combinations in a sunscreen. *International Journal of Pharmaceutics, 307*(2), 123-128.

Giammatteo, M., Cipriani, N., Corona, L., Magaldi, D., Pantaleoni,G. (1997). Osservazioni sull'origine e la composizione chimicomineralogica delle ''terre sigillate'' dell'Isola di Samo. *Miner. Petrogr. Acta* 327 – 337.

Gomes, C. S. F., & Silva, J. B. P. (2007). Minerals and clay minerals in medical geology. *Applied Clay Science, 36*(1-3), 4-21.

Gupta, R. K., & Bhattacharya, S. N. (2008). Polymer-clay nanocomposites: Current status and challenges. *Indian Chemical Engineer, 50*(3), 242-267.

Hayden, C. G., Roberts, M. S., & Benson, H. A. (1997). Systemic absorption of sunscreen after topical application. *The Lancet, 350*(9081), 863-864.

Hule, R. H., & Pochan, D. J. (2007). Polymer nanocomposites for biomedical applications.

MRS Bulletin, 32, 354-358.

Jang, M., Cai, L., Udeani, G.O., Slowing, K. V., Thomas, C. F., Beecher, C. W., Fong, H. H., Farnsworth, N. R., Kinghorn, A. D., Mehta, R. G., Moon, R. C., & Pezzuto, J. M. (1997). Cancer chemopreventive activity of resveratrol, a natural product derived from grapes. *Science, 275*(5297), 218-220.

Klein, N., Fröhlich, F., & Krief, S. (2008). Geophagy: Soil consumption enhances the bioactivities of plants eaten by chimpanzees. *Naturwissenschaften, 95*(4), 325-331.

Kloprogge, J. T., Komarneni, S., & Amonette, J. E. (1999). Synthesis of smectite clay minerals: A critical review. *Clays and Clay Minerals, 47*(5), 529-554.

Krikorian, V., & Pochan, D. J. (2003). Poly (L-lactic acid)/Layered silicate nanocomposite: Fabrication, characterization and properties. *Chemistry of Materials, 15*(22), 4317-4324.

Langan, S. M., & Collins, P. (2006). Photocontact allergy to oxybenzone and contact allergy to lignocaine and prilocaine. *Contact Dermatitis, 54*(3), 173-174.

Lin, F. H., Lee, Y. H., Jian, C. H., Wong, J. M., & Shieh, M. J. (2002). A study of purified montmorillonite intercalated with 5-fluorouracil as drug carrier. *Biomaterials, 23*(9), 1981-1987.

Lowe, N. J. (2006). An overview of ultraviolet radiation, sunscreens and photo-induced dermatoses. *Dermatologic Clinics, 24*(1), 9-17.

Martin, R. T., Bailey, S. W., Eberel, D. D., Fanning, D. S., Guggenheim, S., Kodama, Pevear, D. R., Srodon, J., & Wicks, F. J. (1991). Report of the clay minerals society nomenclature committee: Revised classification of clay minerals. *Clays and Clay Minerals, 39*(3), 333-335.

Murray, H. H. (2000). Traditional and new applications for kaolin, smectite, and palygorskite: A general overview. *Applied Clay Science, 17*(5-6), 207-221.

National Institute of Health. (1989). NIH consens statement online. *Sunlight, Ultraviolet Radiation and the Skin*, 7, 1-29.

Ølholm, J., Paulsen, S. K., Cullberg, K. B., Richelsen, B., & Pedersen, S. B. (2010). Anti-inflammatory effect of resveratrol on adipokine expression and secretion in human adispose tissue explants. *International Journal of Obesity, 34*(10), 1546-1553.

Pandey, K. B., & Rizvi, S. I. (2010). Resveratrol may protect plasma proteins from oxidation under conditions of oxidative stress in vitro. *Journal of the Brazilian Chemical Society, 21*(5), 909-913.

Patel, H. A., Somani, R. S., Bajaj, H. C., & Jasra, R. V. (2006). Nanoclays for polymer nanocomposites, paints, inks, greases and cosmetics formulations, drug delivery vehicle and waste water treatment. *Bulletin of Materials Science, 28*(2), 133-145.

Perioli, L., Ambrogi, V., Bertini, B., Ricci, M., Nocchetti, M., Latterini, L., & Rossi, C. (2006). Anionic clays for sunscreen agent safe use: Photoprotection, photostability and prevention of their skin penentration. *European Journal of Pharmaceutics and Biopharmaceutics, 62*(2), 185-193.

Perugini, P., Simeoni, S., Scalia, S., Genta, I., Modena, T., Conti, B., & Pavanetto, F. (2002). Effect of nanoparticle encapsulation on the photostability of the sunscreen agent, 2-ethylhexyl-p-methoxycinnamate. *International Journal of Pharmaceutics, 246*(1-2), 37-45.

Pineiro, Z., Palma, M., & Barroso, C. G. (2006). Determination of trans-resveratrol in grapes by pressurised liquid extraction and fast high-performance liquid chromatography.

Journal of Chromatography A, 1110(1-2), 61-65.

Pinnavaia, T. J. (1983). Intercalated clay catalysts. *Science, 220*(4595), 365-371.

Roberston, R. H. S. (1996). Cadavers, choleras and clays. *Mineralogical Society Bulletin, 113*, 3-7.

Scalia, S., Molinari, A., Casolari, A., & Maldotti, A. (2004). Complexation of the sunscreen agent, phenylbenzimidazole sulphonic acid with cyclodextrins: Effect of stability and photo-induced free radical formation. *European Journal of Pharmaceutical Sciences, 22*(4), 241-249.

Schallreuter, K. U., Wood, J. M., Farwell, D. W., Moore, J., & Edwards, H. G. M. (1996). Oxybenzone oxidation following solar irradiation of skin: Photoprotection versus antioxidant inactivation. *Journal of Investigative Dermatology, 106*(3), 583-586.

Shi, G., Rao, L., Yu, H., Xian, H., Yang, H., & Ji, R. (2008). Stabilization and encapsulation of photosensitive resveratrol within yeast cell. *International Journal of Pharmaceutics, 349*(1-2), 83-93.

Silva, R., Almeida, L. M., & Brandao, F. M. (1995). Photoallergy to oxybenzone in cosmetic creams. *Contact Dermatitis, 32*(3), 176.

Suresh, R., Borkar, S.N., Sawant, V. A., Shende, V. S., & Dimble, S. K. (2010). Nanoclay drug delivery system. *International Journal of Pharmaceutical Sciences and Nanotechnology, 3*(2), 901-905.

Touitou, E., & Godin, B. (2008). Skin nonpenetrating sunscreens for cosmetic and pharmaceutical formulations. *Clinics in Dermatology, 26*(4), 375-379.

Vastano, B. C., Chen, Y., Zhu, N., Ho, C., Zhou, Z., & Rosen, R. T. (2000). Isolation and

identification of stilbenes in two varieties of polygonum cuspidatum. *Journal of Agricultural and Food Chemistry, 48*(2), 253-256.

Veniale, F. (1997). Applicazioni e utilizzazioni medico-sanitarie di materiali argillosi (naturali e modificati). In: Morandi, N., Dondi, M. (Eds.), *Argille e Minerali delle Argille. Guida alla Definizione di Caratteristiche e Proprietá per gli Usi Industriali.* Corso di Formazione, Gruppo Ital. AIPEA. Rimini (Italy), pp. 205 – 239.

Veniale, F., Setti, M., Soggetti, F., Lofrano, M., Troilo, F. (1999). Esperimenti di "maturazion" di geomateriali argillosi con acqua sulfurea e salso-bromo-ionica per la preparazione di fanghi ''peloidi'' termali e per trattamenti dermatologici. Atti Simposio ''Argille per fanghi peloidi termali e per trattamenti dermatologici e cosmetici'', Montecatini Terme. *Miner. Petrogr. Acta XLII*, 267 – 275.

Vian, M. A., Tomao, V., Gallet, S., Coulomb, P. O., & Lacombe, J. M. (2005). Simple and rapid method for cis- and trans-resveratrol and piceid isomers determination in wine by high-performance liquid chromatography using Chromolith columns. *Journal of Chromatography A, 1085*(2), 224-229.

Viseras, C., Aguzzi, C., Cerezo, P., & Lopez-Galindo, A. (2007). Uses of clay minerals in semisolid health care and therapeutic products. *Applied Clay Science, 36*(1-3), 37-50.

Viseras, C., Cerezo, P., Sanchez, R., Salcedo, I., & Aguzzi, C. (2010). Current challenges in clay minerals for drug delivery. *Applied Clay Science, 48*(3), 291-295.

Vorhies, J. S., & Gaines, R. R. (2009). Microbial dissolution of clay minerals as a source of iron and silica in marine sediments. *Nature Geoscience, 2*(3), 221-225.

Wu, C., Gaharwar, A.K., Schexnailder, P. J., & Schmidt, G. (2010). Development of

biomedical polymer-silicate nanocomposites: A materials science perspective. *Materials, 3*(5), 2986-3005.

Yaar, M. M., & Gilchrest, B. A. (2007). Photoageing: Mechanism, prevention and therapy. *British Journal of Dermatology, 157*(5), 874-887.

Yariv, S., & Michaelian, K. H. (2002). Structure and surface acidity of clay minerals. In S. Yariv & H. Cross (Eds.), *Organo-Clay Complexes and Interactions* (pp. 1-38). New York: Marcel Dekker.

Zhang, X. M., Nakagawa, M., Kawai, K., & Kawai, K. (1998). Erythema-multiforme-like eruption following photoallergic contact dermatitis from oxybenzone. *Contact Dermatitis, 38*(1), 43-44.

Ziegler, A., Jonason, A. S., Leffell, D. J., Simon, J. A., Sharma, H. W., Kimmelman, J., Remington, L., Jacks, T., & Brash, D. E. (1994). Sunburn and p53 in the onset of skin cancer. *Nature, 372*(6508), 773-776.

Chapter 2

Major Techniques of Characterization

2.1 X-ray Diffraction

X-ray diffraction is the most common technique in the study of clay minerals. The scattered waves that result from the impingement of an X-ray beam upon clay minerals may be in phase with one another, forming a wavefront, resulting in constructive interference and consequently diffraction. The Bragg equation relates the wavelength of the X-rays (λ), the glancing angle of incidence (θ), and the interplanar spacing of the crystal, and states the conditions necessary for diffraction (Wilson, 1987).

$$n\lambda = 2d\sin\theta$$

Figure 6 reveals x-rays of wavelength λ impinging onto the layered surface of the crystal at angle θ. Rays OQ and O'A are scattered off the upper layer in the directions QP and AP', arriving at PP' in phase with one another because their path length is the same. When ray O penetrates the surface to reflect off of the lower layer, it travels a distance of 2 BC farther than ray O' which only scatters of the upper layer. In order for the Bragg equation to be satisfied, this path distance of 2BC must be equal to an integer number of wavelengths, n. When this condition is satisfied, the scattered rays CP'' and AP' will be in phase with one another, resulting in constructive interference and diffraction (Wilson, 1987).

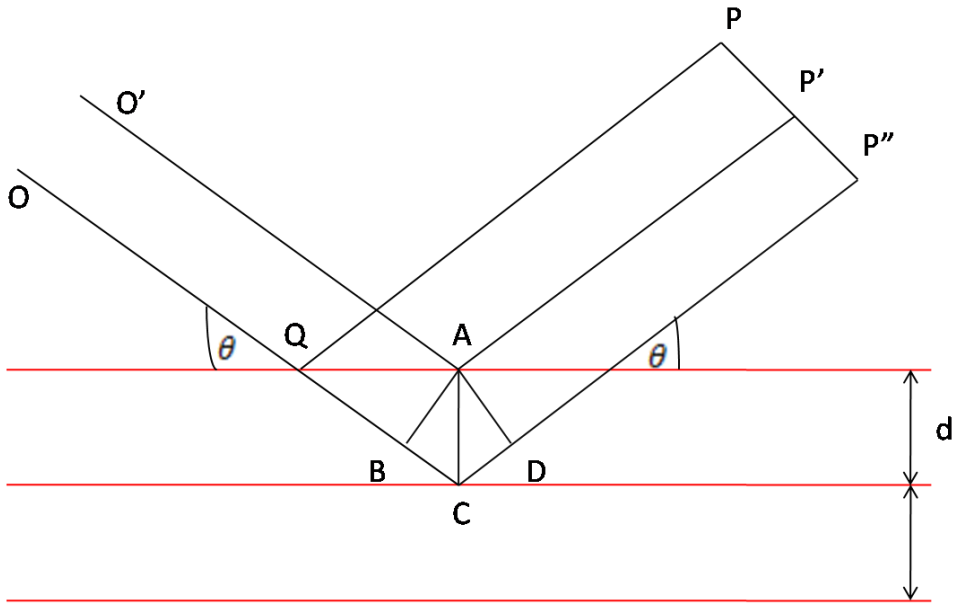

Figure 6. X-ray diffraction from a layer structure (Adapted from Wilson, 1987).

A unified approach to describing analytical instruments, proposed by G. Rayson (2004), and used by McMahon (2008), will be applied, by which each analytical instrument is described as being composed of five distinct modules: source, sample, discriminator, detector and output device. Based on this approach, the schematic diagram (Fig. 7), which represents the X-ray diffractometer, depicts the X-ray tube or synchrotron as the source. The X-rays are generated in a cathode ray tube when a filament is heated, and the generated electrons are made to bombard a target material by the application of a voltage. The monochromator is depicted as the discriminator, which through filtering, produces monochromatic X-rays. The position sensitive counter serves as the detector and registers the diffraction pattern of the sample by moving around the sample. The diffraction data is recorded, manipulated and plotted (McMahon, 2008).

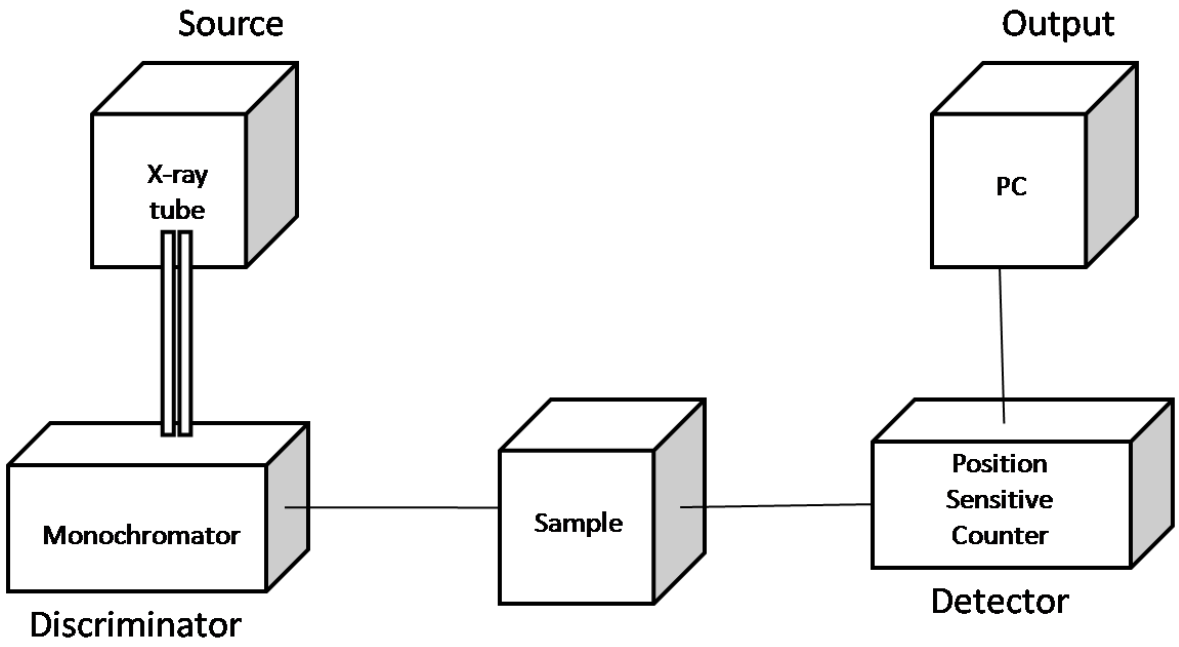

Figure 7. Schematic representation of an X-ray diffraction instrument (Adapted from McMahon, 2008).

Upon the intercalation of clay minerals, there is an expansion in the *c* direction which can be monitored by the basal spacing. When the clay particles are oriented with their basal planes parallel to the plane surface of the diffractometer, an enhancement of the intensity of the 001 reflection is obtained, allowing the reflection to be identified with more certainty. Moreover, the basal spacing is an excellent characteristic for the purposes of differentiating between various clay minerals. The most commonly used technique to achieve this orientation involves pipetting the clay-water suspension onto a microscope slide. Upon drying, the specimens obtained are oriented with the basal plane parallel to the plane of the diffractometer, and are termed ordered aggregates (Nagelschmidt, 1941).

2.2 Thermogravimetric Analysis

The techniques of thermal analysis are defined by the International Confederation for Thermal Analysis and Calorimetry (ICTAC) as those that subject a sample to a programmed temperature in a specified atmosphere while physical or chemical properties of said sample are monitored. The study of clay minerals through the use of thermal analysis techniques dates back to 1887 when Le Chatelier heated samples of clay and used the point of dehydration as a differentiating factor. A major milestone was achieved at the end of the 19^{th} century with the invention of the thermocouple. The joining of two thermocouples was significant since the total voltage produced indicated the difference in temperature of the two thermocouples (Plante *et al.*, 2009). With progressive improvements made over time, thermal analysis techniques have become informative means to study characteristic clay mineral reactions such as dehydration, dehydroxylation, and phase transitions, as well as the thermal reactions of the organic components of organically-modified clay (Langier-Kuzniarowa, 2002; Plante *et al.*, 2009).

Thermogravimetry and derivative thermogravimetry are among the techniques widely used in the study of clay minerals. These thermal techniques require the continuous weighing of a sample, loaded on a high precision thermobalance, while it undergoes a specific thermal program (Plante *et al.*, 2009). A schematic diagram of the thermobalance is illustrated in Figure 8. Sample and reference pan are both attached to the balance, which is enclosed to allow for a controlled atmosphere. The purpose of the reference pan is to offset the weight of the sample pan. Both the reference and sample pan are placed in a high temperature furnace and undergo identical thermal cycles (Thomas & Schmidt, 2010).

Based on the schematic diagram, the source provides the furnace temperature, the temperature program, and other details of the heating cycle. The balance, depicted in the schematic diagram as the discriminator, measures the mass loss with the electromagnetism as the basis of the measurement (McMahon, 2008). A thermocouple is placed in close proximity to the sample in order to allow temperature measurements to be made while mass changes occur (Thomas & Schmidt, 2010). The balance detects the mass change under the influence of temperature and this data is sent to a PC which manipulates the data, plots the TG curves and calculates a DTG curve if required (McMahon, 2008).

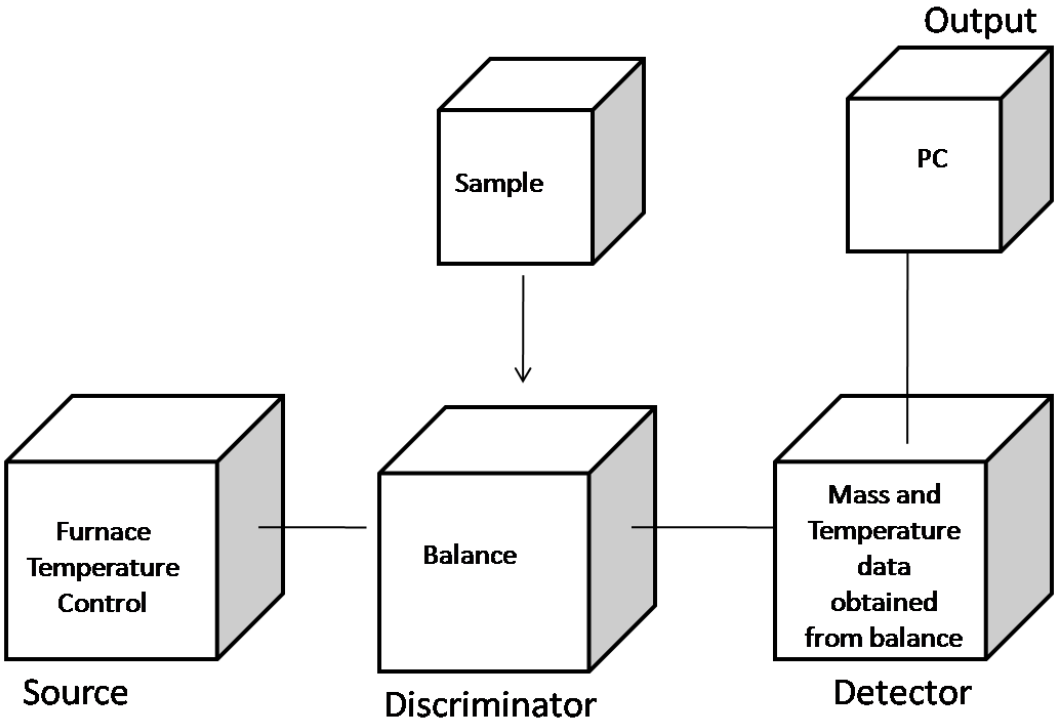

Figure 8. Schematic representation of a thermobalance (Adapted from McMahon, 2008).

The results of the TG analysis are usually documented in a graphical manner. Between the inflection points of the TG curve, the mass loss corresponding to a certain reaction may be measured. Derivative thermogravimetry (DTG), a thermoanalytical technique which provides the first derivative of the TG curve with respect to temperature, allows for a simple and less convoluted manner of interpreting thermal events since it provides an enhanced resolution of the inflection points (Plante *et al.*, 2009).

TG and DTG analysis are useful tools for the analysis of organically-modified clay complexes. An organic compound complexed with clay will often show differing thermal behaviour than the neat organic compound. Changes such as differing intensities, peak shifts and absence of peaks are often exhibited by the complexed organic compound (Langier-Kuzniarowa, 2002). Pristine clay and organically-modified clay undergo a low temperature mass loss associated with the evolution of water from the complex. This may occur due to the loss of exterior water and the loss of interlayer water (Guggenheim, 2001). Clay minerals such as smectite and kaolinite undergo these events in the temperature range of range of ambient to 300℃

The dehydroxylation of clay minerals is another characteristic feature of the thermal behaviour of clay. This is an endothermic event that occurs within the temperature range of 500 - 800℃ and involves the loss of OH groups. In many cases, organo-clay complexes exhibit a lowering of the dehydroxylation temperature of clay minerals, usually by a difference of 30 - 90℃. This has been reported for both kaolinitic clay and smectites, although an explanation has still not been successfully elucidated (Langier-Kuzniarowa, 2002).

2.3 Nuclear magnetic resonance spectroscopy

NMR spectroscopy plays an important role in the investigation of nanocomposite materials by providing detailed knowledge of the structure of its constituents (Geppi *et al.*, 2009). NMR spectroscopy deals with the interaction between the magnetic moment μ_n of nuclei with an external magnetic field (Sanz & Serratosa, 2001). Upon the application of an external magnetic field, a magnetic moment precession and the splitting of the energy levels of the nuclei into 2I + 1 states ensues. As the field strength is increased, the energy separation between the states increases, since they are proportional. When a lower energy state nucleus absorbs a photon of electromagnetic energy, equal to the energy separation between the two states, a flip to the antiparallel orientation occurs and nuclear magnetic resonance is attained (Afremow, 1972; Gerstein, 1994). A signal is produced through the absorption of the photon of energy, and is amplified and recorded (Pahari & Chauhan, 2006).

A schematic of an NMR instrument is illustrated in Figure 9. The sample is placed in the probe, and irradiated by the radiofrequency transmitters (RF Transmitters), depicted on the diagram as the source. When the resonance condition is met, the NMR signal is collected at the radiofrequency receivers (RF receivers), depicted as the detector. NMR signals need to be amplified and processed, and so the free induction decay spectrum in the time domain is recorded and converted into the frequency domain by Fourier transformation (McMahon, 2008).

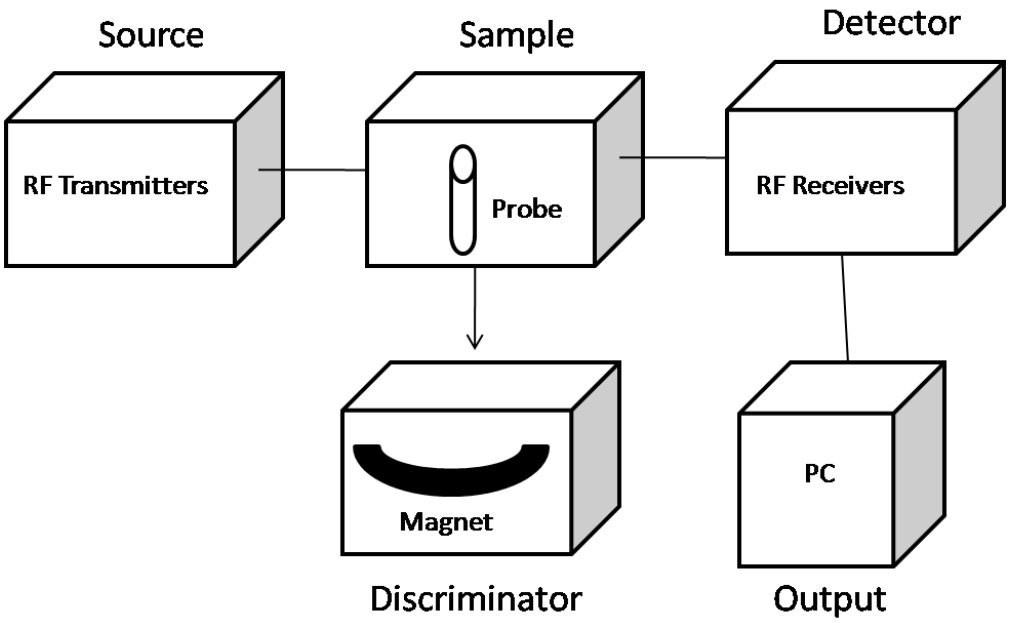

Figure 9. Schematic representation of an NMR spectrometer (Adapted from McMahon, 2008).

The use of solid-state NMR is associated with line broadening and the obscurity of the spectral features. Since the effect of the magnetic field is said to be anisotropic or orientation-dependent, the line broadening occurs due to the variety of possible orientations of molecules in a rigid lattice. On the other hand, with liquids, there is rapid random tumbling that averages out the anisotropic interactions such as dipolar coupling and chemical shift anisotropy. Techniques have been developed and are widely used to improve the resolution of solid-state NMR spectra. The technique known as magic angle spinning (MAS) reduces line broadening and improves the resolution of the spectra (Chmelka & Pines, 1989; Sanz & Serratosa, 2001). This technique involves rapid rotation of the sample at 54.74˚(the magic angle), relative to the static magnetic field (Chmelka & Pines, 1989). At this angle, the average of the geometric term in nuclear spin interactions $(\mathbf{3cos^2\theta - 1}) = \mathbf{0}$,

thereby eliminating the effects of anisotropic interactions (Iggo et al., 2007). Another technique commonly applied to solid-state NMR, often used along with MAS, is cross polarization. This technique involves the transfer of the polarization from abundant nuclei possessing a high gyromagnetic ratio, such as ^{1}H, to dilute nuclei with a low gyromagnetic ratio, such as ^{13}C. This results in a significant signal enhancement (Klinowski, 1985).

2.4 Transmission Electron Microscopy

The transmission electron microscope (TEM) is a high resolution instrument which provides information concerning the sizes and shapes of clay particles and aggregates (Elsass, 2006). The ability to examine the interior of the materials with appropriate resolution makes the TEM an imperative instrument for use in the characterisation of nanomaterials (Ramesh, 2009).

This technique is based on the wavelike character possessed by electrons, as depicted by the following equation:

$$\lambda = \frac{h}{p} = h/(mv)$$

Where $h = 6.626 \text{ x } 10^{-34}$ Js is the Planck constant; p, m and v represent the momentum, mass and speed of the electron (Egerton, 2002). The high energy electrons that are formed can penetrate into a solid, interacting with it as they pass through, thereby projecting both the external surface and the internal surface (Williams & Carter, 2009).

A TEM instrument can be depicted as shown in Figure 10. The source of the electrons is the electron gun. From a heated filament, the electrons are emitted from vacuum and accelerated through a potential difference. The controller serves as the discriminator and is used to scan through the sample. The detector is the phosphor image screen, on which the electrons that have been transmitted through the specimen strike (McMahon, 2008). The scattering process of electrons is a primary factor in image formation. Prior to penetration of the sample, the electron beam has a uniform intensity and travels in a certain direction. In the absence of sample, the electron beam will strike the phosphor screen with a uniform intensity. With the presence of a sample, the spatial uniformity in intensity is affected due to

the scattering process, leading to the appearance of contrast in the images of the specimen. Moreover, an angular variation in intensity leads to the formation of diffraction patterns (Ravishankar, 2010; Williams & Carter, 2009).

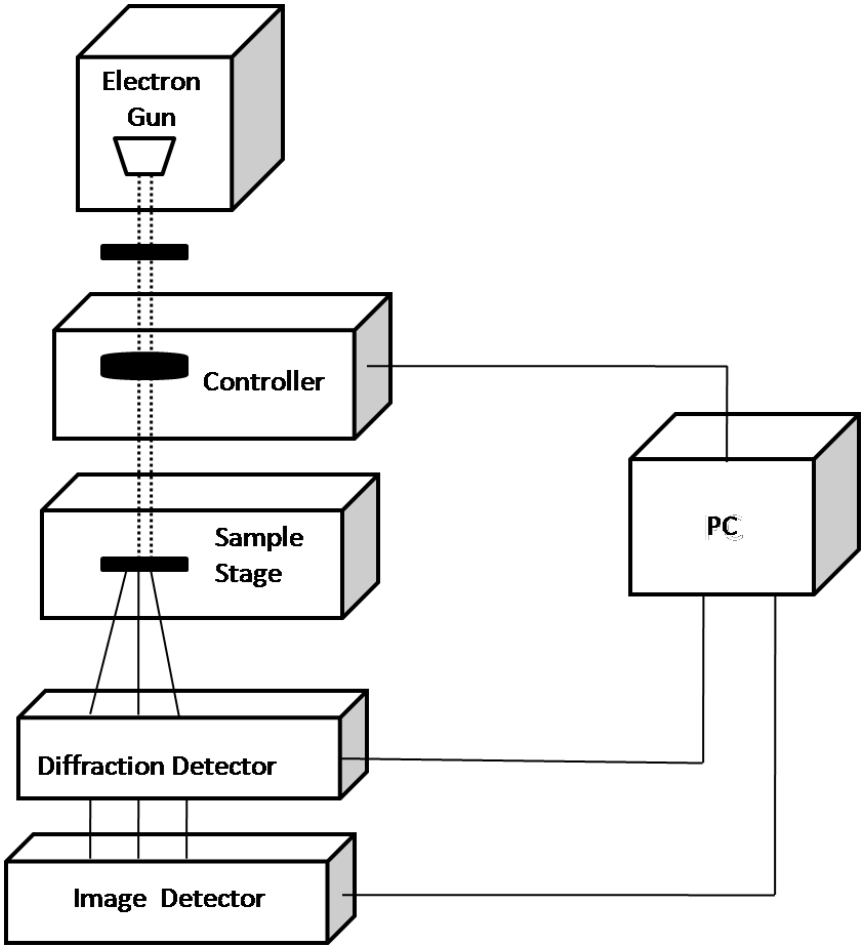

Figure 10. Schematic representation of a transmission electron microscope (Adapted from McMahon, 2008).

References

Afremow, L. C. (1972). Nuclear magnetic resonance spectroscopy. In G. G. Sward (Ed.), *Paint testing manual, physical and chemical examination of paints, varnishes, lacquers, and colors* (13th ed., pp. 564-573). Lutherville-Timonium, MD: American Society for Testing and Materials.

Chmelka, B. F., & Pines, A. (1989). Some developments in nuclear magnetic resonance of solids. *Science, 246*(4926), 71-77.

Egerton, R. F. (2002). *Physical principles of electron microscopy: An introduction to TEM, SEM and AEM.* New York, NY: Springer.

Elsass, F. (2006). Transmission electron microscopy. In F. Bergaya, B. K. G. Theng & G. Lagaly (Eds.), *Handbook of Clay Science* (pp. 939-963). Amsterdam: Elsevier Science.

Geppi, M., Borsacchi, S., Mollica, G., & Veracini, C. A. (2009). Applications of solid-state NMR to the study of organic/inorganic multicomponent materials. *Applied Spectroscopy Reviews, 44*(1), 1-89.

Gerstein, M. (1994). Purcell's role in the discovery of nuclear magnetic resonance: Contingency versus inevitability. *American Journal of Physics, 62*(7), 596.

Guggenheim, S. (2001). Baseline studies of the clay minerals society source clays: Thermal analysis. *Clays and Clay Minerals, 49*(5), 433-443.

Iggo, J. A., Liu, J., & Khimyak, Y. Z. (2007). Nuclear magnetic resonance (NMR) spectroscopy of Inorganic/Organometallic molecules. In A. R. Scott, & M. C.

Lukehart (Eds.), *Applications of physical methods to inorganic and bioinorganic chemistry* (pp. 315-353). West Sussex, England: Wiley-Interscience.

Klinowski, J. (1985). Magic-angle-spinning NMR. *Solid State Ionics, 16*, 3-14.

Langier-Kuzniarowa, A. (2002). Thermal analysis of organo-clay complexes. In S. Yariv, & H. Cross (Eds.), *Organo-Clay Complexes and Interactions* (pp. 273-344) New York: Marcel Dekker.

McMahon. G. (2008). *Analytical instrumentation: A guide to laboratory, portable and miniaturized instruments*. West Sussex, England: Wiley-Interscience.

Nagelschmidt. G. (1941). The identification of clay minerals by means of aggregate x-ray diffraction diagrams. *Journal of Scientific Instruments (1950*), *18*(5), 100-101.

Pahari, A. K., & Chauhan, B. S. (2006). *Engineering chemistry*. New Delhi: Laxmi Publications.

Plante, A. F., Fernandez, J. M., & Leifeld, J. (2009). Application of thermal analysis techniques in soil science. *Geoderma, 153*(1-2), 1-10.

Ramesh, K. T. (2009). *Nanomaterials: Mechanics and mechanisms*. New York: Springer.

Ravishankar, N. (2010). Seeing is believing: Electron microscopy for investigating nanostructures. *The Journal of Physical Chemistry Letters, 1*(8), 1212-1220.

Rayson, G. (2004). A unifying description of modern analytical instrumentation within a course on instrumental methods of analysis. *Journal of Chemical Education, 8*(12), 1767-1771.

Sanz, J., & Serratosa, J. M. (2001). Nuclear magnetic resonance spectroscopy of organo-clay complexes. In S. Yariv, & H. Cross (Eds.), *Organo-Clay Complexes and Interactions* (pp. 223-266). New York: Marcel Dekker.

Thomas, L. C., & Schmidt, S. J. (2010). Thermal analysis. In S. Nielsen (Ed.), *Food analysis* (4th ed., pp. 555-571). New York: Springer.

Williams, D. B., & Carter, C. B. (2009). *Transmission electron microscopy* (2nd ed.). New York: Springer.

Wilson, M J. (1987). X-ray powder diffraction methods. In M. J. Wilson (Ed.), *A handbook of determinative methods in clay mineralogy* (pp. 26-94). New York : Chapman and Hall.

Chapter 3

Adsorption by alkylammonium-modified montmorillonite

3.1 Introduction

Several prominent discoveries compile the history of organically-modified clay, beginning with a paper from Smith in 1934 reporting the saturation of bentonite with nicotine (Smith, 1934). Gieseking's work in 1939 on methylene blue brought to light the ability to replace the positive ions located between the silicate layers. It became known that, in comparison to inorganic positive ions, the large organic ions, such as methylene blue, are held more firmly by the clay (Gieseking, 1939; Hendricks, 1941). The possibility of using alkylammonium ions, currently a commonly used technique for the organic modification of clay, was birthed from this work (De Paiva *et al.*, 2008; Hendricks, 1941). In 1944, MacEwan was seeking a means to identify montmorillonite with ease and discovered that treatment with glycerol resulted in its intercalation into the interlayer region of montmorillonite, and the intercalation was identified by a sharp first-order basal reflection obtained at 1.77 nm (MacEwan, 1944). In 1949, Jordan investigated the preparation of bentonite with aliphatic ammonium salts, forming organophilic bentonite, which has a greater affinity for organic compounds than pristine clay, as well as swelling ability in several organic liquids (Jordan, 1949). Since then, countless studies have been performed on numerous types of organically- modified clay, termed organoclays. Organoclays find uses in many facets of industry including, but not limited to, adsorbents of organic pollutants, rheological control agents, paints and cosmetics (De Paiva *et al.*, 2008).

Montmorillonite is a 2:1 layered clay mineral. Due to extensive isomorphous substitutions, montmorillonite possesses a high negative surface charge, along with charge compensating cations which are exchangeable (Segad *et al.*, 2010; Theng, 1979). The majority of the cations are located within the interlayer space of montmorillonite (Bhiwankar & Weiss, 2005; Theng, 1979). These cations are hydrated, rendering montmorillonite a swelling clay and consequently an extensively studied clay mineral (Bhiwankar & Weiss, 2005; Yariv & Michaelian, 2002). Intercalation of a wide range of molecules within the interlayer space of montmorillonite is possible due to the high swelling capacity which exposes the guest molecules to a large active area (Halim *et al.*, 2010).

Montmorillonite can be modified via different routes of preparation and the success of the modification relies on the interactions that the organic compound can have with the clay mineral. The intercalation into montmorillonite, which requires the penetration of the interlayer space by the guest molecules, can occur via 3 possible mechanisms of interaction: (1) cationic bonding, which commonly involves alkylammonium ions being exchanged with the interlayer sodium cations. (2) Ion-dipole interactions, where polar organic molecules interact with the interlayer sodium cations. (3) Dipole–dipole, interactions where polar organic molecules are hydrogen bonded to oxygen atoms on the basal plane of the clay layer (De Paiva *et al.*, 2008; Dang *et al.*, 2010; Roychand *et al.*, 2010; Su & Thurøcarstensen, 1972; Theng, 1972). Intercalation into untreated montmorillonite is often limited. The most predominantly used organic compounds for the purposes of the preparation of organoclays are quaternary alkylammonium salts (De Paiva *et al.*, 2008), such as cetyltrimethylammonium bromide (CTAB) (Fig. 11).

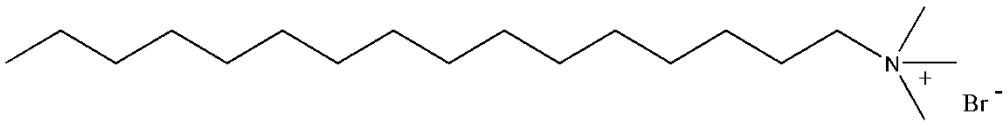

Figure 11. Structure of cetyltrimethylammonium bromide.

Along with attributing organophilic characteristics to the clay, modification with long chain quaternary ammonium salts results in the exposure of new sorption sites on the clay, and increases the interlamellar spacing, all of which are favourable for the adsorption of a secondary compound (Dakovi *et al.*, 2003; Huskić and Žigon, 2009). The adsorption properties possessed by organoclays have stimulated research in the field of water treatment, on account of the ability to remove oil and grease (Beall, 2003). Along with the adsorption of neutral organic contaminants, organically-modified clay has also been researched for use in the fields of drug delivery and cosmetics (Akçay, 2006; Floody *et al.*, 2009; Fu & Qutubuddin, 2001).

Oxybenzone, 2-hydroxy-4-methoxybenzophenone (Fig. 3) (pg. 8), is a frequently used UV filter and a reported photoallergen (Antoniou *et al.*, 2008; Collins & Ferguson, 1994; Langan & Collins, 2006; Silva *et al.*, 1995; Zhang *et al.*, 1998). Encapsulation of active sunscreen ingredients has been studied as a means to reduce allergic reactions due to the avoidance of a direct contact between the sunscreen ingredient and the skin (Perioli *et al.*, 2006; Antoniou *et al.*, 2008; Gaspar & Campos, 2006). Intercalation into the interlayer space of clay minerals can serve as that barrier, whereby the sunscreen ingredient is embedded within the layered structure of clay. Intercalation into the interlayer space of clay may also be advantageous for compounds that lack stability, such as resveratrol (Fig. 4)

(pg. 9), a phenolic compound researched for attributing a multitude of beneficial health effects (Shi *et al.*, 2008). Organically-modified clay, prepared using montmorillonite and cetyltrimethylammonium bromide (CTAB), was fully characterized and was examined for the intercalation of oxybenzone and resveratrol.

3.2 Materials and Techniques of Characterization

Materials

CTAB was purchased from Sigma-Aldrich and used as received. Oxybenzone was purchased from Sigma-Aldrich and used as received. Resveratrol was purchased from BetaPharma Inc. and used as received. Montmorillonite SWy-2 was obtained from the Clay Minerals Society, located at Purdue University, West Lafayette, Indiana, USA. It was purified by the conventional method as follows: montmorillonite was suspended in deionized water and allowed to sediment. The top fraction was collected, and then sodium-saturated by dispersion in 1M NaCl solution, followed by centrifugation to recuperate the clay. The clay was then washed in deionized water followed by centrifugation for recuperation. This process of sodium exchange followed by washing was repeated 4 times. The clay was dialysed in dialysis bags to remove the excess salt. The fine fraction (< 2 μm) of the clay sample was obtained by dispersing the sodium-saturated clay in deionized water in dilute suspensions for 1 week followed by retrieval of the fine fraction on top of the sediment (Carrado *et al.*, 2006).

Techniques of Characterization

X-ray diffraction patterns were obtained on a Philips PW 3710 diffractometer, with a CuKα radiation at a wavelength of 0.154 nm, a generator voltage of 45 kV and current of 40 mA. Thermogravimetric analysis (TG) data were recorded using an SDT 2960 instrument under N_2 flow (120 mL/min) with a heating rate of 10ºC/min. Solid-state ^{13}C CP-MAS NMR spectra were collected using a Bruker AVANCE 200 NMR spectrometer.

3.3 Experimental Procedures

Modification of montmorillonite with alkylammonium (CTA-MMT).

The preparation of CTA-MMT involved first dispersing 2.0 g of Na^+ MMT into 250 mL of water, followed by stirring for 2 hours. 100 mL of a 0.5 M aqueous solution of CTAB was added to the clay dispersion and was magnetically stirred at room temperature for 2 days. The product was recuperated through four cycles of washing/centrifuging using water and centrifuging at 3500 rpm for 3 minutes. The product was dried at 30ºC for 4 hours and then ground into a powder using a mortar and pestle.

Modification of CTA-MMT with oxybenzone (OXY + CTA-MMT).

The preparation of OXY + CTA-MMT involved first dissolving 1g of oxybenzone in 150 mL of methanol, followed by the addition of 0.5 g of CTA-MMT. The resultant dispersion was magnetically stirred at room temperature for 5 days. The product was recuperated through four cycles of washing/centrifuging using methanol and centrifuging at 3500 rpm for 3 minutes. The product was dried at 50ºC for 2 hours and then ground into a powder using a mortar and pestle.

Modification attempt of CTA-MMT with resveratrol (RESV + CTA-MMT).

The preparation of RESV + CTA-MMT involved first dissolving 1 g of resveratrol in 150 mL of methanol followed by the addition of 0.5 g of CTA-MMT. The resultant dispersion was magnetically stirred at room temperature for 5 days. The product was recuperated through four cycles of washing/centrifuging using methanol and centrifuging at

3500 rpm for 3 minutes. The product was dried at 50ºC for 2 hours and then ground into a powder using a mortar and pestle.

CTA-MMT BLANK.

A blank experiment was performed where 0.5 g of CTA-MMT was dispersed in 150 mL of methanol for 5 days, while undergoing magnetic stirring. The product was recuperated through four cycles of washing/centrifuging using methanol and centrifuging at 3500 rpm for 3 minutes. The product was dried at 50ºC for 2 hours and then ground into a powder using a mortar and pestle.

3.4 Results and Discussion

Figure 12 shows the XRD patterns of Na^+ MMT and CTA-MMT. The primary indicator for intercalation is the shift of the 001 reflection from a higher diffraction angle to a lower diffraction angle, indicating an increase in the basal spacing according to Bragg's law. The characteristic 001 reflection of montmorillonite is shifted from 1.19 nm for Na^+ MMT to 1.91 nm for CTA-MMT, indicating an intercalation of the alkylammonium within the interlayer space. The structure of the resultant organoclay, in particular, the interlayer orientation of alkylammonium, is influenced by the length of the alkyl tail. The basal spacing of the resultant modified montmorillonite allows for the elucidation of the interlayer orientation of the surfactant (Lagaly, 1981; Liu *et al.*, 2007; Feng *et al.*, 2009).

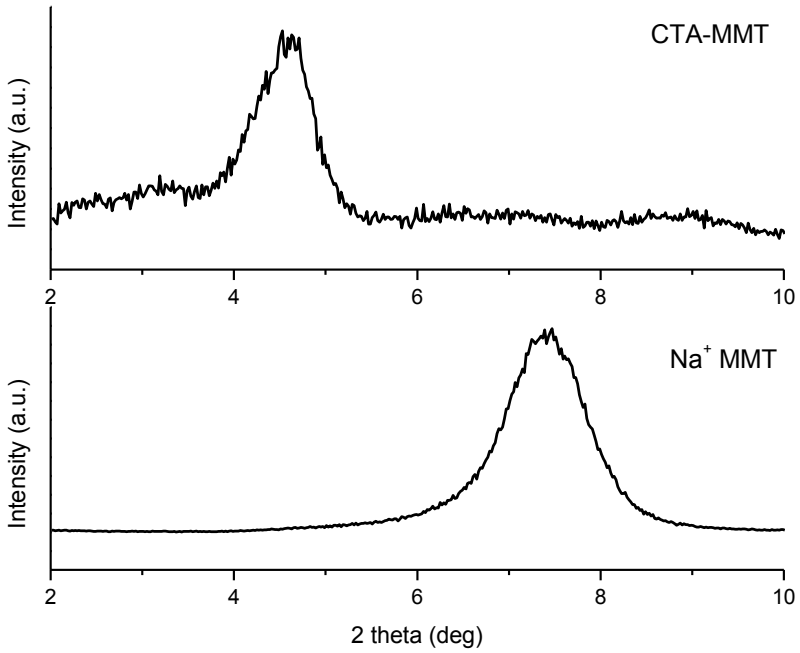

Figure 12. XRD patterns of Na^+ MMT and CTA-MMT.

The subtraction of the thickness of the silicate layer (0.95 nm) from the basal spacing calculates the interlamellar spacing (Ruiz-Hitzky *et al.,* 2005). According to the model proposed by Lagaly & Weiss (1971), and cited by Qi *et al.* (2007), monolayer, bilayer, pseudotrimolecular, or paraffin-type arrangements are possible in the interlamellar space of montmorillonite.

A monolayer arrangement (d_{001} ~ 1.35 nm) indicates an orientation of surfactant within the interlamellar space where the chains lie flat along the clay surface with the alkyl chains parallel to the clay layer (Lagaly *et al.*, 2006; Hrachova *et al.*, 2010). This orientation is the ideal arrangement for alkylammonium ions with short chains (Lagaly *et al.*, 2006). A bilayer orientation (d_{001} ~1.76 nm), also involves the chains lying flat along the clay surface with the alkyl chain parallel to the clay layer (Lagaly, *et al.*, 2006; Hrachova *et al.*, 2010). This orientation is ideal for alkylammonium ions with longer chains such as CTA (Lagaly *et al.*, 2006). A paraffinic- arrangement (d_{001} >2.20 nm) involves an orientation where the alkyl chains are standing in a tilted possession (Lagaly *et al.,* 2006; Hrachova *et al.,* 2010; Frost *et al.,* 2007). A basal spacing of 2.17 nm is in accordance with the pseudotrimolecular arrangement (Lagaly *et al.,* 2006; Hrachova *et al.,* 2010). The 001 reflection for CTA-MMT is 1.91 nm; it is difficult to determine the exact arrangement of the alkyl chains within the interlayer since such basal spacing values are in between those reported for bilayer arrangements and pseudotrimolecular layer arrangements, and correspond to an interstratification of the bilayer and pseudotrimolecular layer complexes (Ogawa *et al.*, 1995; Ramirez *et al*., 2005).

Electrostatic forces cause the attraction of the organic cations to the negatively charged montmorillonite layers. Maximum neutralization of the organic cation occurs in the

interlamellar space due to the negative charge possessed by the clay layers. Further attributing to the intercalation, van der Waals forces exist between the oxygen of the oxygen plane of montmorillonite and the organic compound in the interlayer space. Adsorption beyond the CEC may also occur, which involves an intercalation of the surfactant with the anion counterpart as an ion pair, and is driven by van der Waals interactions between alkyl chains (Yariv, 2002).

Thermal analysis is a conventional technique for the characterization of organoclays. The thermal treatment of unmodified montmorillonite occurs through a characteristic two – step decomposition process, as revealed by thermogravimetric analysis (Fig. 13).

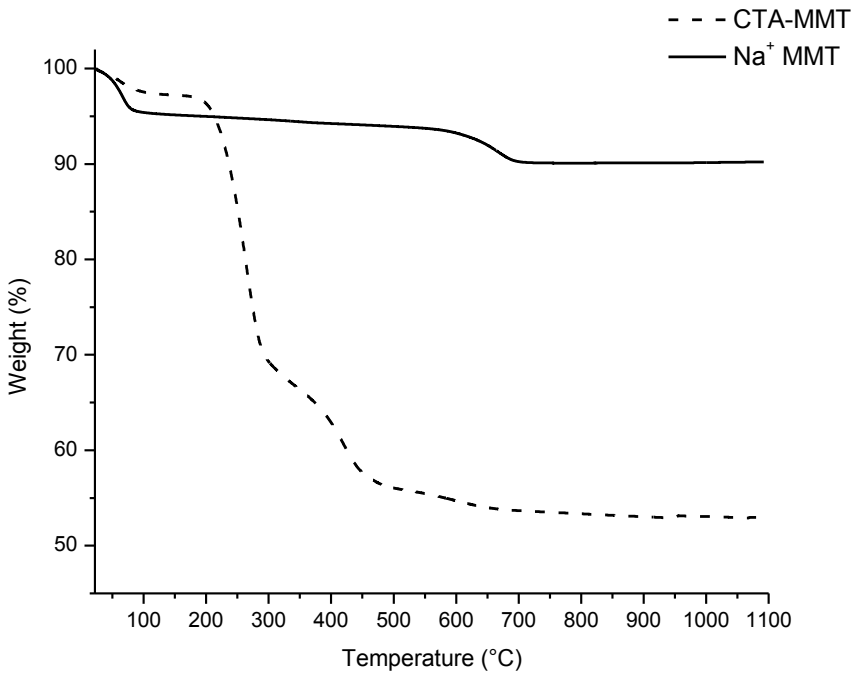

Figure 13. TG traces of Na^+ MMT and CTA-MMT.

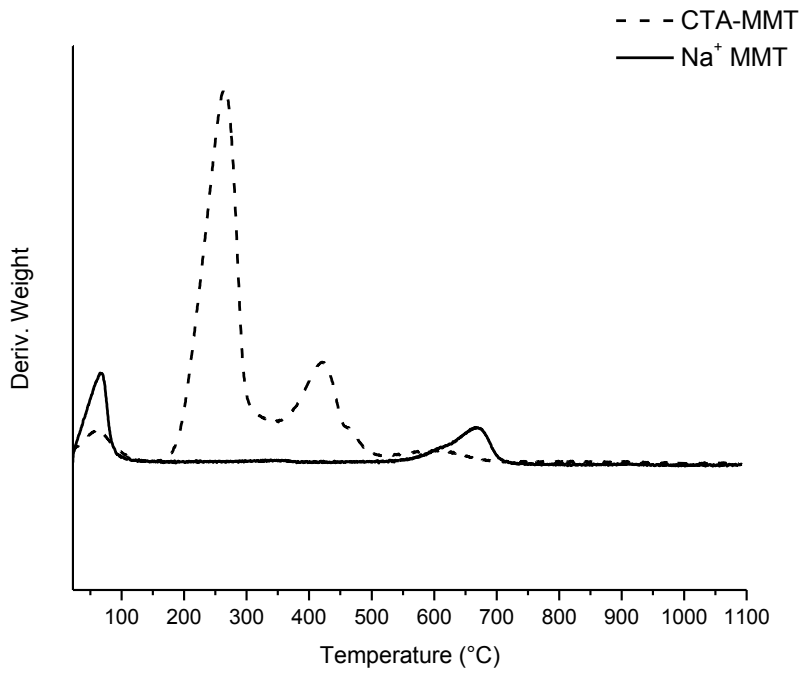

Figure 14. DTG traces of Na^+ MMT and CTA-MMT.

The TG trace for Na^+ MMT reveals a total weight loss of 9.63%, with the first weight loss occurring within the temperature range of 25℃ - 100℃, which corresponds to the desorption of water. The corresponding peak in the DTG trace (Fig. 14) is broad, indicating the different environments of water existing in montmorillonite; weakly bound water, adsorbed to the surfaces of crystals and free water pockets located within the aggregate structure, evaporate within the lower temperature range, while interlamellar water, along with water of the hydration sphere of the interlamellar sodium cations, evaporate within the higher temperature range. The second weight loss step which occurs within the temperature range of 560℃ - 700℃, corresponds to the loss of structural water, a process known as the dehydroxylation of clay minerals, also evidenced as a broad peak on the DTG trace (Hoidy *et al.*, 2009; Xie *et al.*, 2001)

The intercalation of CTA-MMT is characterized by analysis of the TG trace (Fig. 13). The total weight loss for CTA-MMT is 37.3% greater than the total weight loss for Na^+ MMT. The DTG trace of CTA-MMT (Fig. 14) reveals the decomposition occurring in accordance with the thermal decomposition of a typical quaternary alkylammonium-modified montmorillonite (Hoidy *et al.*, 2009; Xie *et al.*, 2001). The first weight loss step, as observed on the DTG trace within the temperature range of 25℃ – 100℃, corresponds to the desorption of water. Although alkylammonium-modified montmorillonite is considered hydrophobic, a desorption of water resulting from thermal treatment is expected due to the water adsorption that occurs along the layer edges and on the exterior surfaces of aggregates (Xie *et al.*, 2001; Langier-Kuzniarowa, 2002). The second and third weight losses are observed within the ranges of 180℃ - 340℃ and 340℃ - 500℃, respectively, and are attributed to the loss of the alkylammonium. The loss of the alkylammonium in multiple steps indicates different types of bonding within the organoclay (Langier-Kuzniarowa, 2002). The weight loss within the temperature range of 340℃ - 500℃, observed on the DTG trace as a peak centered at 420℃, accounts for the loss of alkylammonium chains interacting electrostatically with the clay surface. The weight loss observed within the temperature range of 180℃ - 340℃, observed on the DTG trace as a peak centered at 260℃, includes the loss of weakly held alkylammonium, located on the exterior of the layers and/or interacting via van der Waals interactions with the other alkylammonium chains (Xi *et al.*, 2005).

The attempt to intercalate resveratrol in CTA-MMT was performed by dispersing CTA-MMT in a solution of resveratrol in methanol. In order for an accurate comparison to

be made, the blank experiment was performed where CTA-MMT was suspended in methanol and stirred for 5 days.

Analysis of the XRD pattern of the blank experiment (Fig. 15) reveals a shift of the 001 reflection from 1.91 nm to 1.79 nm, indicating an interlamellar spacing of 0.84 nm, which corresponds to a bilayer orientation of the alkylammonium ions in the interlamellar space. The decrease in the interlamellar space corresponds to a desorption of alkylammonium ions from the interstratified bilayer/pseudotrimolecular layer complex with a rearrangement of the adsorbed surfactant to form a bilayer complex. The desorption likely involves the surfactant in excess of the CEC that is retained by van der Waals interactions, and exude a lesser stability than the surfactant retained by cationic exchange (Li & Jian, 2009; Ni *et al.*, 2009; Xi *et al.*, 2005).

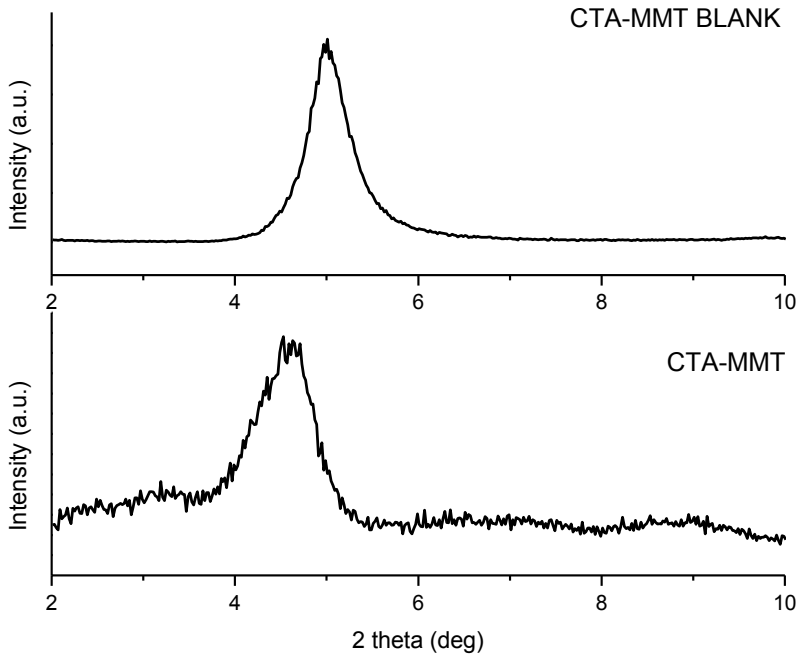

Figure 15. XRD patterns of CTA-MMT and CTA-MMT BLANK.

When CTA-MMT was dispersed in a solution of resveratrol and washed by the conventional technique of centrifugation, the sample acquired (RESV + CTA-MMT) displays an XRD pattern (Fig. 16) very similar to that of CTA-MMT BLANK , with a 001 reflection centered at 1.79 nm. This indicates that the dispersion of CTA-MMT in a solution of resveratrol results in the desorption of weakly bound surfactant in excess of the CEC, and a rearrangement of the adsorbed surfactant into a bilayer complex. For secondary adsorption onto organoclay, a lack of expansion of the interlayer space may result, despite the occurrence of intercalation (Lagaly *et a.l*, 2006; Xu & Boyd, 1995). Therefore, determining whether intercalation occurs requires additional characterization techniques.

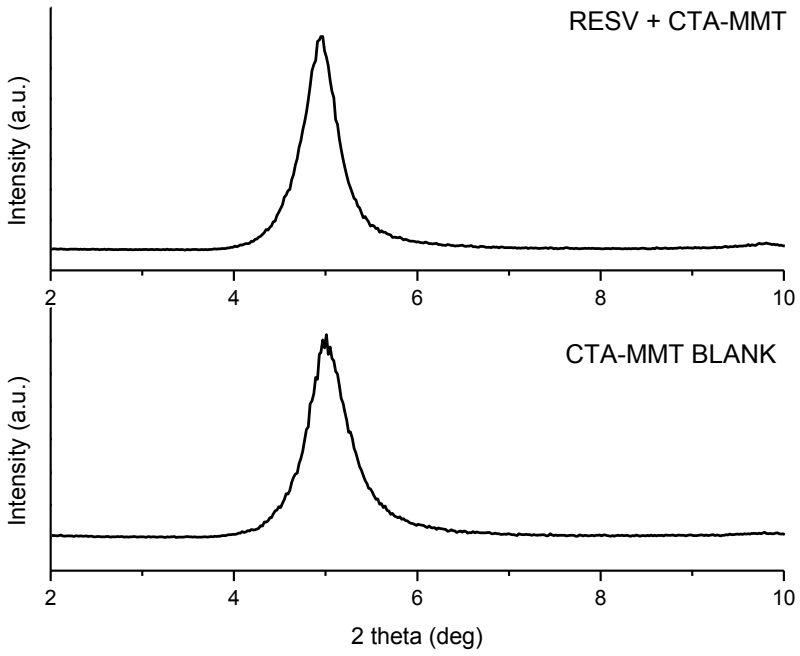

Figure 16. XRD patterns of CTA-MMT BLANK and RESV + CTA-MMT.

Figure 17 indicates the DTG traces of RESV + CTA-MMT and CTA- MMT BLANK. The DTG trace of CTA-MMT BLANK indicates the signature weight losses of an

alkylammonium-modified clay, beginning with the desorption of water within the temperature range of 25℃ - 100℃. This is followed by the second weight loss, which is a two step process occurring within the ranges of 200℃ - 340℃ and 340℃ - 500℃, with DTG peaks centered at 300℃ and 420℃, respectively, and is attributed to the loss of the surfactant. The dehydroxylation of montmorillonite constitutes the final weight loss occurring within the temperature range of 530℃ - 680℃. The thermal behaviour of RESV+ CTA-MMT appears to be parallel to that of CTA-MMT BLANK, as revealed by their similar TG traces (Fig. 18) and DTG traces (Fig. 17). Moreover, the total weight loss of CTA-MMT BLANK (29.4 %) is very similar in value to that of RESV + CTA-MMT (28.1%) indicating the lack of adsorption of resveratrol.

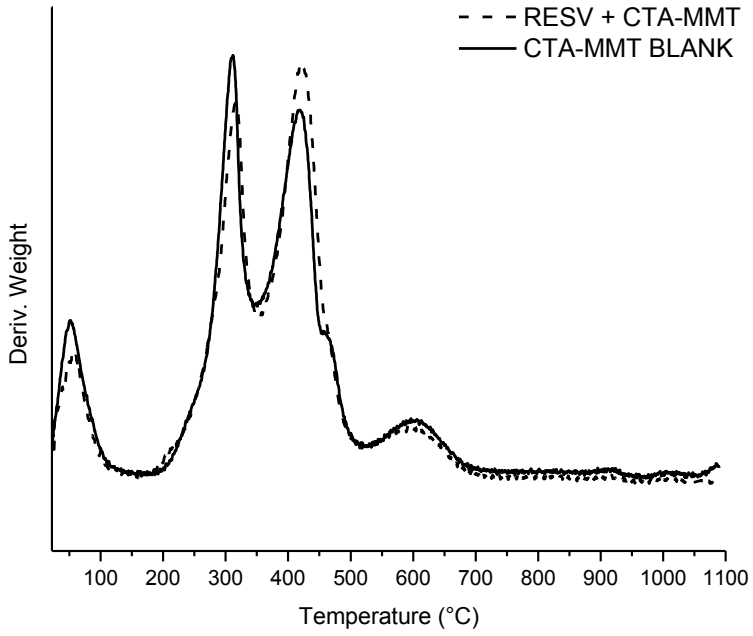

Figure 17. DTG traces of CTA-MMT BLANK and RESV + CTA-MMT.

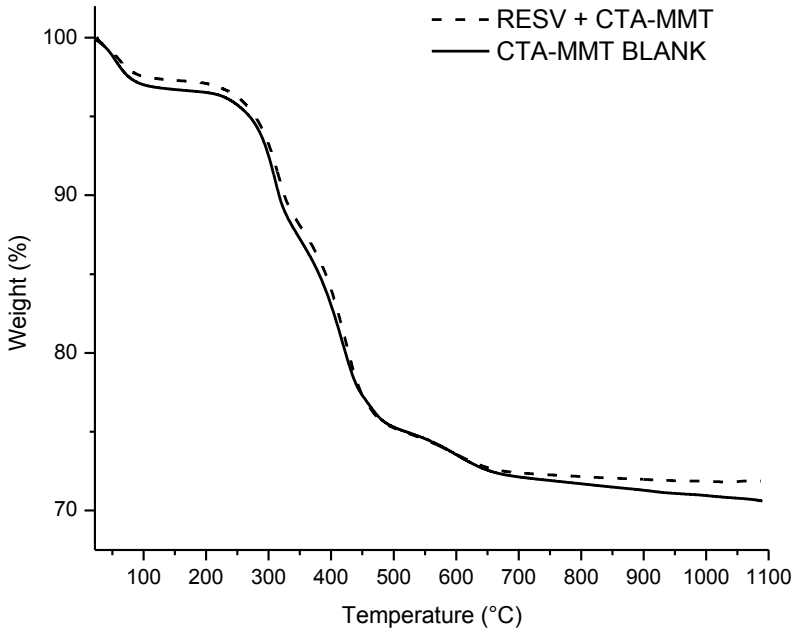

Figure 18. TG traces of CTA-MMT BLANK and RESV+CTA-MMT.

When CTA-MMT was dispersed in a solution of oxybenzone and washed by the conventional technique of centrifugation, the sample acquired (OXY + CTA-MMT) displays an XRD pattern (Fig. 19) also very similar to that of CTA-MMT BLANK, with a 001 reflection centered at 1.79 nm. This indicates that the dispersion of CTA-MMT in a solution of oxybenzone also results in a desorption of weakly bound surfactant in excess of the CEC and a rearrangement of the adsorbed surfactant into a bilayer complex. For secondary adsorption onto organoclay, a lack of expansion of the interlayer space may result, despite the occurrence of intercalation (Lagaly *et al.*, 2006; Xu and Boyd, 1995). Thermal analysis techniques are required to determine whether intercalation of oxybenzone occurred.

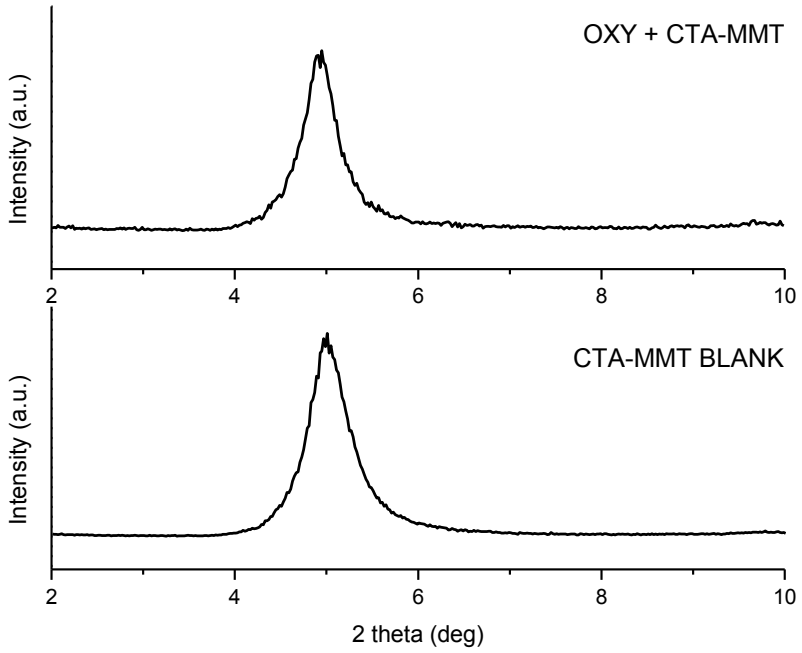

Figure 19. XRD patterns of CTA-MMT BLANK and OXY+ CTA-MMT.

Analysis of TG data indicates the adsorption of oxybenzone by the modified-montmorillonite CTA-MMT. The TG trace of OXY + CTA-MMT (Fig. 20) indicates a total weight loss of 36.2% while the blank experiment reveals a lesser total weight loss of 29.4%.

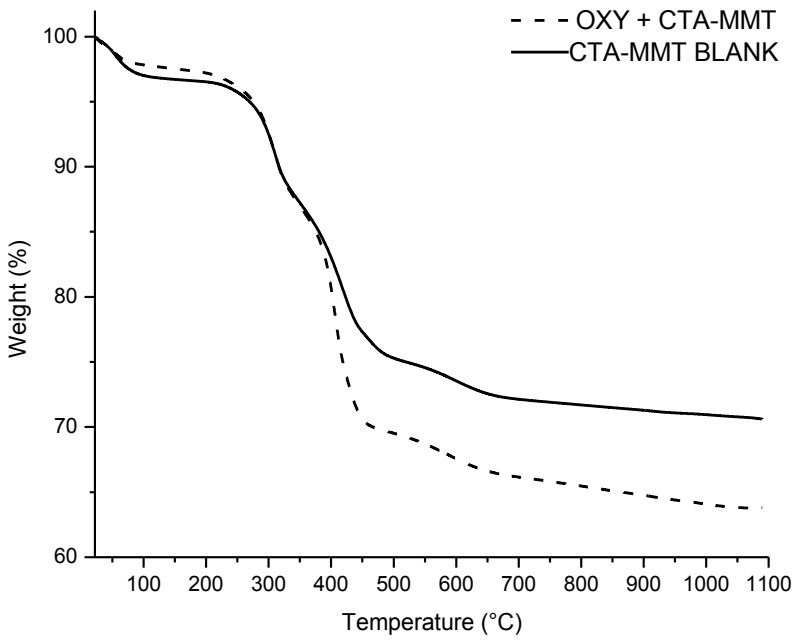

Figure 20. TG traces of CTA-MMT BLANK and OXY+ CTA-MMT.

The comparison of the DTG traces of CTA-MMT BLANK and OXY + CTA-MMT reveals a marked difference (Fig. 21). The DTG trace for CTA-MMT BLANK indicates the decomposition of surfactant by 2 steps: the first peak is centered at 300℃ and the second peak is centered at 420℃ with a small shoulder at 470℃. In the case of OXY + CTA-MMT, the loss of organic also occurs by two steps: the first peak is centered at 300℃, and correlates very well with the corresponding peak in CTA-MMT BLANK. The second peak for the loss of organic in OXY+ CTA-MMT, centered at 405℃, reveals a significant increase in intensity, relative to the peak centered at 420℃ for CTA-MMT BLANK. The increase in intensity of the peak is likely due to the thermal decomposition of oxybenzone. The onset of decomposition of oxybenzone is 180℃ for the pure compound

and is concluded at 290℃ (Fig. 22) and so the adsorption of oxybenzone likely led to an increase in its thermal stability, resulting in the onset of its decomposition at a higher temperature.

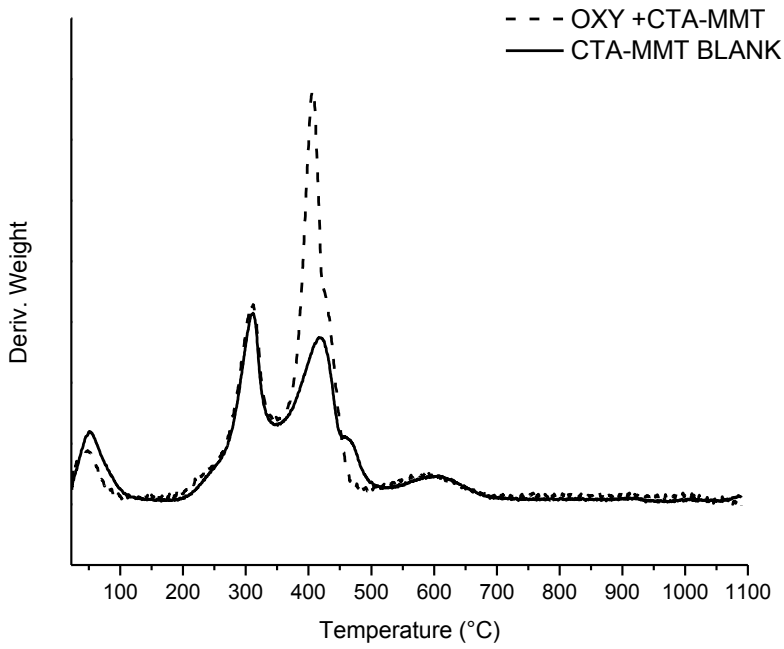

Figure 21. DTG traces of CTA-MMT BLANK and OXY+ CTA-MMT.

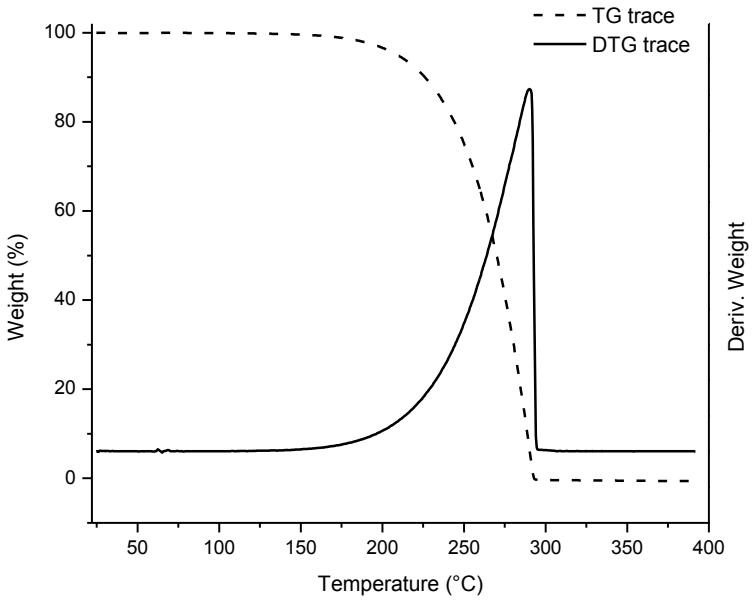

Figure 22. TG and DTG traces of oxybenzone.

Therefore it can be reasonably concluded that the increase in intensity seen in the DTG trace and the increase in the total weight loss seen in the TG trace for OXY+ CTA-MMT, as compared to the blank experiment, is a result of the adsorbed oxybenzone.

Analysis of the ^{13}C CP-MAS NMR spectrum of OXY + CTA-MMT indicates that the signals are broader than those seen in the spectra of CTA-MMT BLANK and CTA-MMT (Fig. 23). In the case of CTA-MMT, the signals arise from both the intercalated species as well as the portion attached to the external montmorillonite surfaces (Lagaly *et al.*, 2006; Theng *et al.*, 1998). In the case of CTA-MMT BLANK, which has undergone a treatment to desorb the externally adsorbed portion of surfactant, the signals arise primarily due to the intercalated species. The spectrum for CTA-MMT BLANK reveals a resolution comparable to that of CTA-MMT, with assignable peaks. The broadness of the peaks

corresponding to CTA, in the case of OXY + CTA-MMT is significant since this would indicate a more disordered structure than in CTA-MMT BLANK or CTA-MMT. The intercalation of oxybenzone presumably occurs due to hydrophobic interactions with the alkyl chain. Therefore, the conformation of the interlamellar surfactant is expected to be perturbed due to a mixing with the oxybenzone molecules, resulting in a more disordered structure than in CTA-MMT BLANK or CTA-MMT. The chemical shift dispersion that occurs upon intercalation was noted by Theng *et al.* (1998) and Elbokl & Detellier (2008). Moreover, a broad peak within the aromatic region can be seen in the spectrum for OXY + CTA-MMT, further corroborating the uptake of oxybenzone by CTA-MMT.

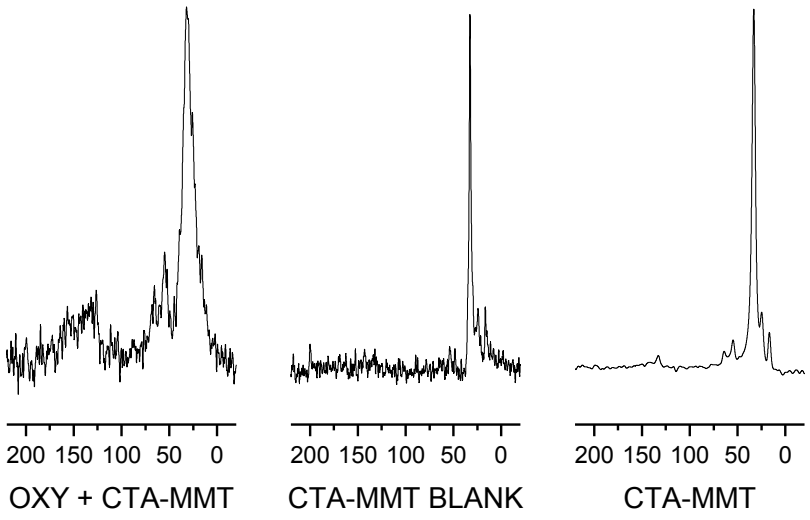

Figure 23. ^{13}C CP-MAS NMR spectra of OXY+CTA-MMT, CTA-MMT BLANK and CTA-MMT.

Several phenomena must be taken into consideration when studying the secondary adsorption of neutral molecules by clays previously modified with organic cations. Unlike primary, secondary or tertiary ammonium ions, whereby hydrogen bonding with water molecules is possible, quaternary ammonium ions are incapable of being proton donors (Yariv, 2002). Consequently the intercalation of quaternary ammonium cations results in eliminating the limitations imposed by a hydrophilic environment (Theng *et al.*, 1998). Intercalated cationic surfactants act as a pillar, enhancing the interlamellar space by propping open the clay layers and spatially accommodating the intercalation of a secondary compound such as oxybenzone (Yariv, 2002). In addition, swelling of the modified clay favours the intercalation process. The intercalation medium used was methanol which is capable of solvating the hydrocarbon chains of the interlamellar surfactant resulting in swelling. This allows for effective oxybenzone movement into the interlayer region, favouring the intercalation process (Nzengung *et al.*, 1996; Slabaugh & Hiltner, 1968).

Potential sites for the adsorption of neutral organic compounds include both the siloxane surfaces and the alkylammonium compounds (Akçay, 2006). In the case of montmorillonite modified with small organic cations such as tetramethylammonium, the siloxane surface is available as an adsorption site since neither the cation nor its hydration waters completely occupy the interlamellar environment (Roberts *et al*., 2006). Oxybenzone, a hydrophobic compound (Sarp *et al.*, 2009), is likely adsorbed by CTA-MMT via van der Waals interactions with the alkyl chains belonging to the alkylammonium within the interlamellar space (Erim & Alemdar, 1998; Roberts *et al.*, 2006).

As determined by ICP-MS results (Table 1), the cation exchange capacity of the montmorillonite used is determined to be 74.5meq/100g, according to the sodium, potassium

and calcium concentration of the sample, which is in excellent agreement with the cation exchange capacity of SWy-2 provided by the producer (76.4 meq/100 g), as cited by *Xi et al.*, 2005.

Concentration (ppm)	**Ca**	**K**	**Na**
Na^+ MMT	339	201	16625

Table 1. ICP-MS determined concentrations of various ions present in Na^+ MMT.

TG results provide a means of relating the organic content of the sample CTA-MMT with the cation exchange capacity (meq/100g of MMT); this can determine whether the CTA was adsorbed in excess of the CEC (Ganguly *et al.*, 2010). As described by Ganguly *et al.* (2010), the following calculation was performed using TG data within the temperature range of 100℃- 1100℃:

Let clay show x % weight loss.

Let CTA-MMT show y % weight loss.

Let CTA-MMT show n % organic loading.

Therefore, weight loss from 100g of modified clay $(y) = \frac{n+\{(100-n)*x\}}{100}$

$n = \frac{\{100*(y-x)\}}{100-x}$

% organic loading $(z) = \frac{(n*100)}{(100-n)}$

Meq/100g of clay $= \left\{\frac{z}{(\text{Molecular Weight of CTA})} * 1000\right\}$

The amount of CTA adsorbed onto montmorillonite was calculated to be approximately 3.4 times the CEC of Na^+ MMT. The CTA content of the CTA-MMT

BLANK sample is approximately 1.4 times the CEC, indicating a desorption of alkylammonium, in comparison to CTA-MMT.

Under the assumption that the ratio of CTA:MMT is the same in both CTA-MMT BLANK and OXY + CTA-MMT, and based on TGA results within the temperature range of 100-1100℃, the loading of oxybenzone onto 100g of modified clay is determined to be approximately 10.1g. The ratio of CTA:OXY in the sample OXY + CTA-MMT is 2.4:1.

The OXY+ CTA-MMT sample was thoroughly washed through centrifugation, ensuring the removal of any surface adsorbed molecules, and so it is plausible to conclude that an adsorption of oxybenzone occurred through an intercalation. The d_{001} peak corresponds to an interlamellar space of 0.84 nm, identical to that of CTA-MMT BLANK which means that the oxybenzone occupied gaps existing within the interlamellar space caused by the intercalation of surfactant.

3. 5 Conclusion

An organoclay prepared using cetyltrimethylammonium and montmorillonite exhibited an adsorption capability for oxybenzone, a frequently used UV filter. The complex and its precursor were fully characterized using the conventional techniques of XRD, TG and DTG analysis and ^{13}C CP-MAS NMR. Based on previous studies conducted on the adsorption of secondary compounds by organoclay, the adsorption of a secondary compound was facilitated possibly due to the expansion of the interlamellar space, a conversion of the interlamellar properties from hydrophilic to hydrophobic, and the endowment of the clay with sorption sites suitable for the uptake of hydrophobic compounds (Lee & Shackelford, 2005).

References

Akçay, M. (2006). Characterization and adsorption properties of tetrabutylammonium montmorillonite (TBAM) clay: Thermodynamic and kinetic calculations. *Journal of Colloid and Interface Science, 296*(1), 16-21.

Antoniou, C., Kosmadaki, M. G., Stratigos, A. J., & Katsambas, A. D. (2008). Sunscreens-what's important to know. *Journal of the European Academy of Dermatology and Venereology, 22*(9), 1110-1119.

Beall, G. W. (2003). The use of organo-clays in water treatment. *Applied Clay Science, 24*(1-2), 11-20.

Bhiwankar, N. N. & Weiss, R. A. (2005). Melt-intercalation of sodium-montmorillonite with alkylamine and quaternized ammonium salts of sulfonated polystyrene ionomers. *Polymer, 46*(18), 7246-7254.

Carrado, K. A., Decarreau, A., Petit, S., Bergaya, F., & Lagaly, G. (2006). Synthetic clay minerals and purification of natural clays. In F. Bergaya, B. K. G. Theng & G. Lagaly (Eds.), *Handbook of Clay Science* (pp.115-139). Amsterdam: Elsevier.

Collins, P., & Ferguson, J. (1994). Photoallergic contact dermatitis to oxybenzone. *British Journal of Dermatology, 131*(1), 124-129.

Dakovi, A., Toma, A., Rottinghaus, H., Dondur, V., Dondurc, V., & Ma, Z. (2003). Adsorption of ochratoxin A on octadecyldimethyl benzyl ammonium exchanged-clinoptilolite-heulandite tuff. *Colloids and Surfaces B: Biointerfaces, 30*(1-2), 157-165.

Dang, Q., Lu, S., Sun, P., Yuan, Z. (2010). Silk fibroin/montmorillonite nanocomposites:

Effect of pH on the conformation transition and clay dispersion. *Biomacromolecules, 11*(7), 1796-1801.

De Paiva., L. B., Morales, A. R., & Diaz, F. R. V. (2008). Organoclays: Properties, preparation and applications. *Applied Clay Science, 42*(1-2), 8-24.

Elbokl, T. A., & Detellier, C. (2008). Intercalation of cyclic imides in kaolinite. *Journal of Colloid and Interface Science, 323*(2), 338-348.

Erim, F. B. & Alemdar, I. (1998). Preconcentration of phenols by adsorption on organo-clay followed by capillary electrophoretic determination. *Fresenius'Journal of Analytical Chemistry*, *361*(5), 455-458.

Faschan, A., Tittlebaum, M., & Cartledge, F. (1993). Nonionic organic partitioning onto organoclays. *Hazardous Waste Hazardous Materials, 10*(3), 313-322.

Feng, X., Meng, X., Ding, Y., Zhang, S., & Yang, M. (2009). Influence of ethanol addition on the modification of montmorillonite by hexadecyl trimethylammonium bromide. *Applied Clay Science, 45*(4), 239-243.

Floody, M. C., Theng, B. K. G., Reyes, P., & Mora, M. L. (2009). Natural nanoclays: Applications and future trends- A Chilean perspective. *Clay Minerals, 44*(2), 161-176.

Frost, R., Xi, Y., & Hongping, H. (2007). Modification of the surfaces of Wyoming montmorillonite by the cationic surfactants alkyl trimethyl, dialkyl dimethyl and trialkyl methyl ammonium bromides. *Journal of Colloid and Interface Science, 305*(1), 150-158.

Fu, X., & Qutubuddin, S. (2001). Polymer-clay nanocomposites: Exfoliation of organophilic montmorillonite nanolayers in polystyrene. *Polymer, 42*(2), 807-813.

Ganguly, S., Dana, K., & Ghatak, S. (2010). Thermogravimetric study of n-alkylammonium-intercalated montmorillonites of different cation exchange capacity. *Journal of Thermal Analysis* and Calorimetry, 100(1), 71-78.

Gaspar, L. R., & Campos, P. M. B. G. (2006). Evaluation of the photostability of different UV filter combinations in a sunscreen. *International Journal of Pharmaceutics, 307*(2), 123-128.

Gieseking, J. E. (1939). The mechanism of cation exchange in the montmorillonite-beidellite-nontronite type of clay minerals. *Soil Science, 47*(1), 1-14.

Halim, N. A., Ibrahim, A., & Ahmad, A. B. (2010). Intercalation of water and guest molecules within Ca^{2+} montmorillonite: DSC studies in low temperature range. *Journal of Thermal Analysis and Calorimetry, 102*(3), 983-988.

Hendricks, S. B. (1941). Base exchange of the clay mineral montmorillonite for organic cations and its dependence upon adsorption due to van der Waals forces. *Journal of Physical Chemistry, 45*(1), 65-81.

Hoidy, W. H., Mansor, B., Ahmad, E. A., Jaffar, A. M., & Nor, A. B. I. (2009). Synthesis and characterization of organoclay from sodium montmorillonite and fatty hydroxamic acids. *American Journal of Applied Sciences*, *6*(8), 1567-1572.

Hrachova, J., Billik, P., & Fajnor, V. S. (2010). Influence of organic surfactants on structural stability of mechanochemically treated bentonite. *Journal of Thermal Analysis and Calorimetry, 101*, 161-168.

Huskić, M., & Žigon, M. (2009). The effects of experimental parameters on the extent of intercalation of PMMA/MMT nanocomposites prepared in solution. *Journal of Applied Polymer Science, 113*(2), 1182-11187.

Jordan, J. W. (1949). Organophilic bentonites. I. Swelling in organic liquids. *Journal of Physical Chemistry, 53*(2), 294-306.

Kornecki, T. S., Allred, B., & Brown, G. O. (1997). Determination of cationic and anionic surfactant concentrations in soil. *Soil Science. 162*(6) 439-446.

Lagaly, G., Ogawa, M., & Dekany, I. (2006). Clay mineral organic interactions. In F. Bergaya, B. K. G. Theng, & G. Lagaly (Eds.), *Handbook of Clay Science* (pp. 309-377). Amsterdam: Elsevier.

Lagaly, G., & Weiss, A. (1971). Anordnung und orientierung kationischer tenside auf silicatoberflachen IV. Anordnung von n-alkylammoniumionen bein niedrig geladen schichtsilicaten. *Kolloid. Z. Z. Polym., 243,* 48-55.

Lagaly, G. (1981). Characterization of clays by organic compounds. *Clay Minerals, 16*(1), 1-21.

Langan, S. M., & Collins, P. (2006). Photocontact allergy to oxybenzone and contact allergy to lignocaine and prilocaine. *Contact Dermatitis, 54*(3), 173-174.

Langier-Kuzniarowa, A. (2002). Thermal analysis of organo-clay complexes. In S. Yariv, & H. Cross (Eds.), *Organo-clay complexes and interactions* (pp. 273-344). New York: Marcel Dekker.

Lee, J. & Shackelford, C. D. (2005). Impact of bentonite quality on hydraulic conductivity of geosynthetic clay liners. *Journal of Geotechnical and Geoenvironmental Engineering, 131*(1), 64-77.

Li, Z. & Jian, W. (2009). A thermogravimetric investigation of alkylammonium intercalation into rectorite. *Thermochimica Acta, 483*(102), 58-65.

Liu, X., Lu, X., Wang, R., Zhou, H., & Xu, S. (2007). Interlayer structure and dynamics of

alkylammonium-intercalated smectites with and without water: A molecular dynamics study. *Clays and Clay Minerals, 55*(6), 554-564.

MacEwan, D. M. C. (1944). Identification of the montmorillonite group of minerals by X-rays. *Nature, 154*(3914), 577-578.

Ni, R., Huang, Y., & Yao, C. (2009). Thermogravimetric analysis of organoclays intercalated with the Gemini surfactant. *Journal of Thermal Analysis and Calorimetry, 96*(3), 943-947.

Nzengung, V. A., Voudrias, E. A., Nkedi-Kizza, P., Wampler, J. M., & Weaver, C. E. (1996). Organic cosolvent effects on sorption equilibrium of hydrophobic organic chemicals by organoclays. *Environmental Science Technology, 30*(1), 89-96.

Ogawa, M., Wada, T., & Kuroda, K. (1995). Intercalation of pyrene into alkylammonium-exchanged swelling layered silicates: The effects of the arrangements of the interlayer alkylammonium ions on the states of adsorbates. *Langmuir, 11*(11), 4598-4600.

Perioli, L., Ambrogi, V., Bertini, B., Ricci, M., Nocchetti, M., Latterini, L., & Rossi, C. (2006). Anionic clays for sunscreen agent safe use: Photoprotection, photostability and prevention of their skin penetration. *European Journal of Pharmaceutics and Biopharmaceutics, 62*(2), 185-193.

Perugini, P., Simeoni, S., Scalia, S., Genta, I., Modena, T., Conti, B., & Pavanetto, F. (2002). Effect of nanoparticle encapsulation on the photostability of the sunscreen agent, 2-ethylhexyl-p-methoxycinnamate. *International Journal of Pharmaceutics, 246*(1-2), 37-45.

Qi, L., Lia, W., & Zhichu, B. (2007). Adsorption of conventional and gemini surfactants in

nonswelling and swelling layer silicate. *Colloids and Surfaces A: Physicochemical and Engineering Aspects, 302*(1-3), 568-572.

Ramirez, S., Righi, D., & Petit, S. (2005). Alteration of smectites induced by hydrolytic exchange. *Clay Minerals, 40*(1), 15-24.

Roberts, M. G., Li, H., Teppen, B. J., & Boyd, S. A. (2006). Sorption of nitroaromatics by ammonium-and organic ammonium-exchanged smectite: Shift from adsorption/complexation to a partition-dominated process. *Clays and Clay Minerals, 54*(4), 426-434.

Roychand, P., Angove, M., & Tisdall, J. (2010). Sorptive protection of organic matter in soil. *19th World Congress of Soil Science, Soil Solutions for a Changing World,* 235-238.

Ruiz-Hitzky, E., Darder, M., & Aranda, P. (2005). Functional biopolymer nanocomposites based on layered solids. *Journal of Materials Chemistry, 15*(35-36), 3650-3662.

Sarp, S., Lee, S., Park, N., Hanh, N. T., & Cho, J. (2009). Controlling various contaminants in wastewater effluent through membranes and engineered wetland. *Frontiers of Environmental Science Engineering in China, 3*(1), 98-105.

Segad, M., Jönsson, B., Akesson, T., & Cabane, B. (2010). Ca/Na montmorillonite: Structure, forces and swelling properties. *Langmuir, 26*(8), 5782-5790.

Shi, G., Rao, L., Yu, H., Xiang, H., Yang, H., & Ji. R. (2008). Stabilization and encapsulation of photosensitive resveratrol within yeast cell. *International Journal of Pharmaceutics, 349*(1-2). 83-93.

Slabaugh, W. H. & Hiltner, P. A. (1968). The swelling of alkylammonium montmorillonites. *Journal of Physical Chemistry, 72*(12), 4297-4298.

Smith, C. R. (1934). Base exchange reactions of bentonite and salts of organic bases. *Journal of the American Chemical Society, 56*(7), 1561-1563.

Su, K. S., & Thurøcarstensen, J. (1972). Nature of bonding in montmorillonite adsorbates II. Bonding as an ion-dipole interaction. *Journal of Pharmaceutical Sciences, 61*(3), 420-424.

Theng, B. K. G. (1972). Formation, properties, and practical applications of clay-organic complexes. *Journal of the Royal Society of New Zealand, 2*(4), 437-457.

Theng, B. K. G. (1979). *Formation and properties of clay-polymer complexes.* Amsterdam: Elsevier.

Theng, B. K. G., Newman, R. H., & Whitton, J. S. (1998). Characterization of an alkylammonium-montmorillonite-phenanthrene intercalation complex by carbon -13 nuclear magnetic resonance spectroscopy. *Clay Minerals, 33*(2-3), 221-229.

Xi, Y., Martens, W., He, H., & Frost, R. L. (2005). Thermogravimetric analysis of organoclays intercalated with the surfactant octadeyltrimethylammonium bromide. *Journal of Thermal Analysis and Calorimetry, 81*(1), 91-97.

Xie, W., Gao, Z., Pan, W., Huner, D., Singh, A., & Vaia, R. (2001). Thermal degradation chemistry of alkyl quaternary ammonium montmorillonite. *Chemistry of Materials, 13*(9), 2979-2990.

Xu, S., & Boyd, S. A. (1995). Cationic surfactant sorption to a vermiculitic subsoil via hydrophobic bonding. *Environmental Science Technology, 29*(2), 312-320.

Yariv, S. (2002). Introduction to organo-clay complexes and interactions. In S. Yariv & H. Cross (Eds.), *Organo-Clay Complexes and Interactions* (pp. 39-111). New York: Marcel Dekker.

Yariv, S., & Michaelian, K. H. (2002). Structure and surface acidity of clay minerals. In S. Yariv & H. Cross (Eds.), *Organo-Clay Complexes and Interactions* (pp. 1-38). New York: Marcel Dekker.

Chapter 4

Guar-Montmorillonite Nanocomposites

4.1 Introduction

Nanocomposites are defined as solids from the combination of at least two materials containing a continuous phase and a dispersed phase (Ruiz-Hitzky & van Meerbeek, 2006), with at least one phase possessing one nanoscale dimension (Wegner & Jones, 2009).

Polymer/layered silicate nanocomposites are the most intensely researched type of nanocomposites. A large emphasis is placed on polymer/clay nanocomposites, on account of the low cost, environmental friendliness and availability of clay minerals, with montmorillonite as one of the most commonly used layered silicates (Ray & Bousmina, 2005). These nanocomposites are often described as either intercalated or delaminated (Fig. 24). The term intercalated describes the insertion of the polymer chain into the interlayer space of montmorillonite, while maintaining crystallographic order. Delaminated implies disruption of the layer stacking, with separation and dispersion of the individual layers in the polymer matrix (Choudalakis & Gotsis, 2009; Ray & Okamoto, 2003; Ray *et al.*, 2003).

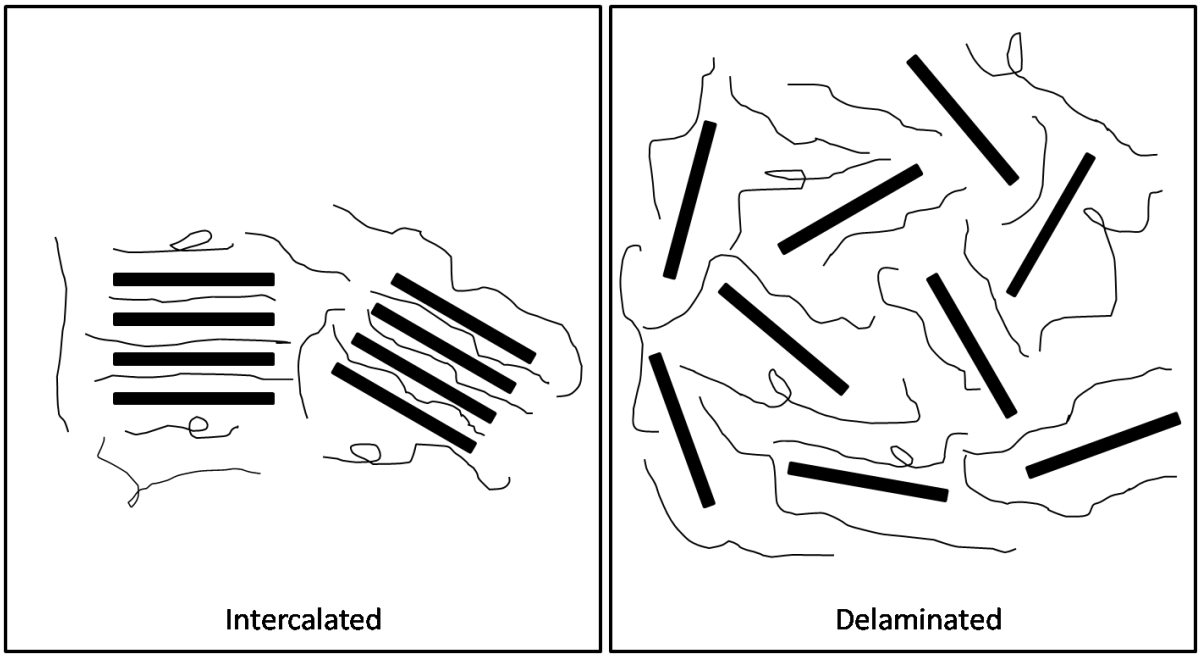

Figure 24. Schematic illustrations of two different types of polymer/layered silicate nanocomposites, (Adapted from Ray *et al.,* 2003).

Polymer/layered silicate nanocomposites (PLS) have a relatively recent history, with the development of the first successful PLS nanocomposite during the 90s by Toyota Central Research & Development Co., Inc. (TCRD). Extensive research in the field prior to the success achieved by TCRD had been performed; however, the inability to achieve a satisfactory dispersion of clay particles in the matrix led to weakened strength and other undesirable properties. In 1987, researchers from TCRD employed the approach of improving the clay's organophilicity by replacing inorganic cations with alkylammonium ions. The resultant organoclays were compatible with hydrophobic polymer matrices. In 1993, an exfoliated nylon 6/layered silicate was developed through the in-situ polymerization of caprolactam in alkylammonium-clay, birthing a new genre of materials

that became known as the polymer/layered silicate nanocomposites (Okamoto, 2005; Ray & Okamoto, 2003).

Polymer/layered silicate nanocomposites are generally prepared by using one of three techniques. One technique involves the intercalation of monomers, followed by polymerization as initiated by heat, radiation, or by the diffusion of a suitable initiator. Another technique, often utilized, is the melt intercalation technique, whereby the polymer chains diffuse into the interlayer space during the annealing process. This technique is especially appealing from an environmental perspective due to the absence of solvent. The third technique is the solvent intercalation method which employs a solvent system capable of dissolving the polymer and swelling the layered silicate. The intercalation of the polymer and layered silicate upon mixing, followed by the removal of the solvent, results in the formation of the polymer/layered silicate nanocomposite (Okamoto, 2005; Ray & Okamoto, 2003; Ray & Bousmina, 2005).

Great interest has been generated in the use of polymer/layered silicate nanocomposites due to a synergism of properties inherent to both the organic and inorganic constituents (Wang *et al.*, 2008), with a potentiality for application in many fields, including drug delivery systems (Campbell *et al.*, 2008). Several examples of montmorillonite modified with synthetic polymers, for the purposes of drug delivery, exist in literature (Wang *et al.*, 2008). For example, the slow release of dexamethasone was achieved using nanocomposites based on poly(ethylene-co-vinyl acetate) and montmorillonite (Cypes *et al.*, 2003). As well, *N*-isopropylacrylamide-montmorillonite nanocomposite hydrogels were synthesized and investigated in terms of physical properties and drug release behaviour for drugs with different charges (Lee & Fu, 2003; Wang *et al.*, 2008).

Biopolymer-modified clay corresponds with an increasing paradigm shift towards green chemistry. The impetus towards natural polysaccharide-modified clay is based on the general biodegradability, environmental friendliness and renewable nature of biopolymers (Rhim & Ng, 2007), which is in accordance with the principles of green chemistry (Park *et al.*, 2004). Moreover, polysaccharides are abundant in nature and available at a low cost (Rhim & Ng, 2007). Among the polysaccharides investigated for the modification of montmorillonite, much interest has been generated in chitosan, due to a control that can be exerted on whether the chitosan intercalates as a monolayer or a bilayer (Ruiz-Hitzky *et al.*, 2005; Ruiz-Hitzky & van Meerbeek, 2006). An acidic medium allows for an exchange of polycationic chitosan with the interlayer cations (Darder *et al*, 2003). Cellulose is another biopolymer capable of forming the polymer-clay nanocomposite, but its lack of solubility in water is a limiting factor (Ruiz-Hitzky *et al.*, 2005).

Plant gums are polysaccharide exudates that can be dissolved or dispersed in water to form viscous solutions or dispersions (Chudzikowski, 1971; Kaplan, 1998). Some gums are pathological products, produced when the plant is subjected to stress (Chudzikowski, 1971; Kreer *et al.*, 2010), and others are due to normal enzymatic activity of the plant (Lapasin & Pricl, 1999). Currently widely used in industry, plant gums were historically particularly important materials. During the third millennium, the ancient Egyptians used plant gums for embalming the dead and for adhering strips together for the purpose of binding mummies. The adhesive properties of gums were taken advantage of during that time period for use as adhesives of mineral pigments in paint formulations used for making hieroglyphics (Chudzikowski, 1971; Verbeken *et al.*, 2003). Moreover, the consumption and the utilization of plant gums for food and medicinal purposes was prevalent amongst many civilizations

(Chudzikowski, 1971). Currently, plant gums are important materials for food, pharmaceutical, paper textile and other industries (Iqbal, 1993).

Guar gum (Fig. 25) is a galactomannan polysaccharide obtained from the endosperm of the seed of *Cyamopsis tetragonoloba*, a plant belonging to the family Leguminosae, where it serves as a food reserve (Levy *et al.*, 1995; Srivastava & Kapoor, 2005). *Cyamopsis tetragonoloba* is an annual pod-bearing plant, about 0.6 m high. It has been cultivated for several thousand years in India and Pakistan (Chudzikowski, 1971). This gum consists of a backbone of (1-4) β-D-manno-pyranosyl, units with every second unit bearing an (1-6) α-D-galacto-pyranosyl unit (Fig. 25) (Gliko-Kabir *et al.*, 1999).

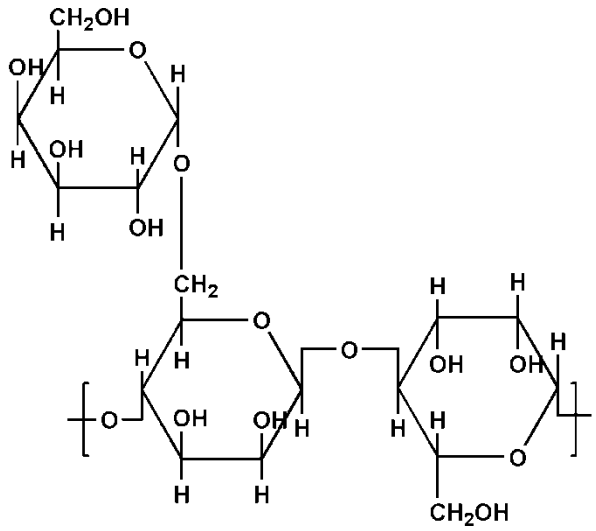

Figure 25. Structure of neutral guar gum.

The neutral form of guar gum (Fig. 25) can be chemically modified to produce a quaternary ammonium compound, guar hydroxypropyltrimonium chloride, also known as cationic guar gum (Fig. 26). This modified gum is used in the paper industry, fibre board

compositions, washing compositions, shampoo solutions and hair-setting compositions (Levy *et al.*, 1995).

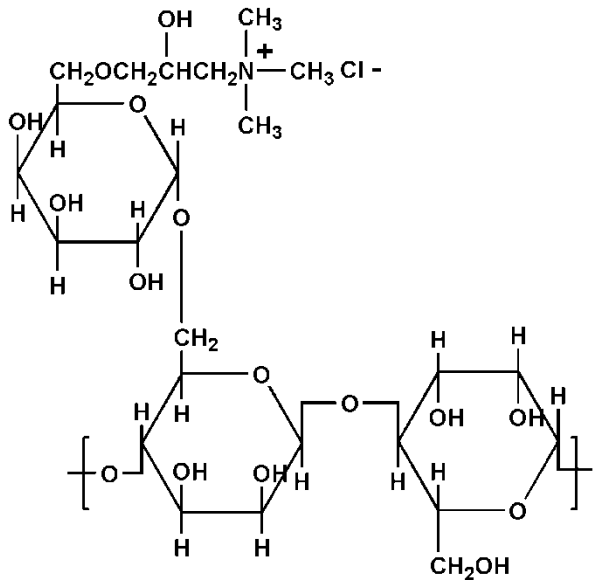

Figure 26. Structure of cationic guar gum.

Neutral guar gum and cationic guar gum are used for the preparation of novel bionanocomposites, with montmorillonite as the inorganic constituent. Polymer nanocomposites are extremely attractive due to the synergism of properties from the parent constituents, forming unique materials with new or significantly enhanced properties that find applications in many facets of industry, ranging from food packing to automotive (Ahmadi *et al.*, 2004; Hule & Pochan, 2007; Oriakhi, 2000). The use of a polysaccharide as the organic constituent, such as guar gum, diversifies the applications by adding the dimension of biodegradability (Hule & Pochan, 2007). Guar-montmorillonite nanocomposites are prepared using an environmentally friendly process and are fully characterized.

4.2 Materials and techniques of characterization

Materials.

Cationic guar gum (CG) was purchased from Spec-Chem Ind. and used as received. Neutral guar gum (NG) was purchased from Sigma-Aldrich and used as received. According to the product specifications by Sigma-Aldrich, the batch of neutral guar gum used possesses a total ash content of ≤1 %. Montmorillonite SWy-2 was obtained from the Clay Minerals Society, located at Purdue University, West Lafayette, Indiana, USA. It was purified by the conventional method as follows: Montmorillonite was suspended in deionized water and allowed to sediment. The top fraction was collected, and then sodium-saturated by dispersion in 1M NaCl solution, followed by centrifugation to recuperate the clay. The clay was then washed in deionized water followed by centrifugation for recuperation. This process of sodium exchange followed by washing was repeated 4 times. The clay was dialysed in dialysis bags to remove the excess salt. The fine fraction (< 2 μm) of the clay sample was obtained by dispersing the sodium-saturated clay in deionized water in dilute suspensions for 1 week followed by retrieval of the fine fraction on top of the sediment (Carrado *et al.*, 2006).

Techniques of Characterization.

X-ray diffraction patterns were obtained on a Philips PW 3710 diffractometer, with a CuKα radiation at a wavelength of 0.154 nm, a generator voltage of 45 kV and current of 40 mA. Thermogravimetric analysis (TG) data were recorded using an SDT 2960 instrument under N_2 flow (120 mL/min) with a heating rate of 10ºC/min. Solid-state ^{13}C CP-MAS

NMR spectra were collected using a Bruker AVANCE 200 NMR spectrometer. Transmission electron microscope images were obtained on a JEOL JEM-2100F electron microscope. The sample, suspended in ethanol, underwent 10 minutes of ultrasonic treatment, and was then deposited as a suspension onto carbon-film-coated copper grids.

4.3 Experimental procedures

Preparation of cationic guar–montmorillonite nanocomposite (CG-MMT 3:1).

The preparation of CG-MMT 3:1 involved first dissolving 9.0 g of cationic guar gum in 1.5 L of water followed by the addition of 3.0 g of Na^+ MMT. The resultant dispersion was stirred at room temperature for 3 weeks. The product was recuperated through four cycles of washing/centrifuging using water and centrifuging at 3500 rpm for 4 minutes. The product was dried at 50 ºC for 4 hours and then ground into a powder using a mortar and pestle.

Preparation of neutral guar–montmorillonite nanocomposites (NG-MMT 3:1 and NG-MMT 6:1).

The preparation of NG-MMT 3:1 involved first dissolving 7.5 g of neutral guar gum in 1.5 L of water followed by the addition of 2.5 g of Na^+ MMT. The resultant dispersion was stirred at room temperature for 3 weeks. The preparation of NG-MMT 6:1 involved first dissolving 15 g of neutral guar gum in 1.5 L of water followed by the addition of 2.5 g of Na^+ MMT. The resultant dispersion was stirred at room temperature for 3 weeks. Both products were recuperated through four cycles of washing/centrifuging using water and centrifuging at 3500 rpm for 4 minutes for each cycle. The products was dried at 50 ºC for 4 hours and then ground into a powder using a mortar and pestle.

Preparation of blank neutral guar experiment (NG BLANK).

A blank experiment was performed where 15 g of neutral guar were dissolved in 1.5 L of water and stirred at room temperature for 3 weeks. This was followed by four cycles of washing/centrifuging using water at 3500 rpm for 4 minutes for each cycle. The product was dried at 50ºC for 4 hours and then ground into a powder using a mortar and pestle.

4.4 Results and Discussion

Figure 27 shows the XRD patterns of CG-MMT 3:1, as compared to starting Na^+ MMT and Figure 28 shows the XRD patterns of NG-MMT 3:1 and NG-MMT 6:1, as compared to starting Na^+ MMT. In the case of CG-MMT 3:1, the enhancement of the d_{001} value from 1.19 nm to 1.40 nm indicates an intercalation of the cationic guar gum. The orientation of intercalated polysaccharide molecules can be deduced from the basal spacing observed. When the thickness of the silicate layer (0.95 nm) is subtracted, a resultant 0.45 nm interlamellar spacing is calculated, which is in accordance with a monolayer orientation (Ruiz-Hitzky *et al*., 2005). In the case of NG-MMT 3:1 and NG-MMT 6:1 (Fig. 28), as compared to starting Na^+ MMT, an enhancement of the d_{001} values can also be seen in both cases, indicating the intercalation of neutral guar gum within the montmorillonite layers. As well, in both cases, there is splitting of the d_{001} diffraction peaks into two peaks, (d_{001} values of $\sim$ 1.37 nm and 1.83 nm), indicating an intercalation of polysaccharides with a monolayer orientation and bilayer orientation, respectively. Interlamellar spacings of 0.42 nm and 0.88 nm, corresponding to a monolayer orientation and bilayer orientation respectively, are deduced by subtracting the thickness of the silicate layer. In the case of NG-MMT 6:1, the bilayer orientation is more predominantly formed, indicating a reliance of the orientation on the concentration of the guar gum in the solvent during the preparation process.

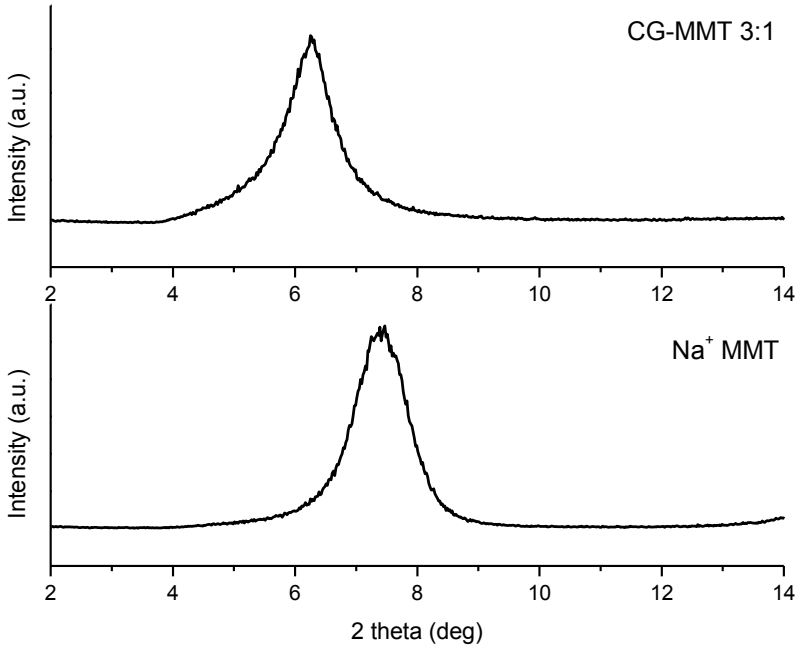

Figure 27. XRD patterns of Na^+ MMT and CG-MMT 3:1

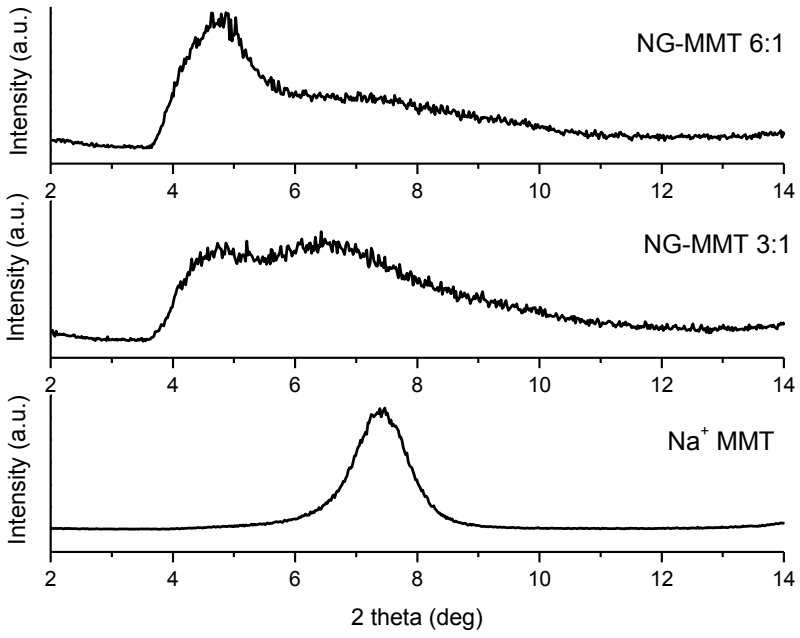

Figure 28. XRD patterns of Na^+ MMT, NG-MMT 3:1 and NG-MMT 6:1

Intercalation is a complex process that can invoke several mechanisms of interaction. The ion-exchange process, which involves maintaining the charge neutralisation of the montmorillonite layers, is dominant in the case of cationic polymers such as cationic guar gum (Theng, 1979). With the intercalation of neutral species, van der Waals forces enable for the stabilization of the species within the interlayer space (Ruiz-Hitzky *et al.*, 2005). Guar gum is laden with hydroxyl groups, thereby offering the potential for hydrogen bonding interactions with the siloxane surfaces. Along with hydrogen bonding and van der Waals interactions, entropy effects are also effective in the intercalation process (De Souza, 2010).

TEM results (Fig. 29) are in good agreement with the XRD results, indicating the intercalation of the cationic guar gum, expanding the interlayer space to approximately 1.4 nm (Fig. 29 C). The intercalation appears to be disordered in certain regions (Fig 29 B), where the extent of interlayer expansion is not consistent, thereby justifying the broadness of the d_{001} peak (Martín *et al.*, 2009). The layers of NG-MMT 3:1 (Fig. 29 D-F) and NG-MMT 6:1 (Fig. 29 G-I) retain their parallel alignment and stack together in domains that range in size from 20-60 nm, indicating intercalation. Moreover, the TEM images reveal that there is a mixed morphology, with the existence of partially delaminated regions indicated by the detachment of a stack of platelets from the edge (Martín *et al.*, 2009). Regions exhibiting layer curvature are clearly seen, indicating the flexibility of the layers as a result of the high aspect ratio (Bhiwankar & Weiss, 2006).

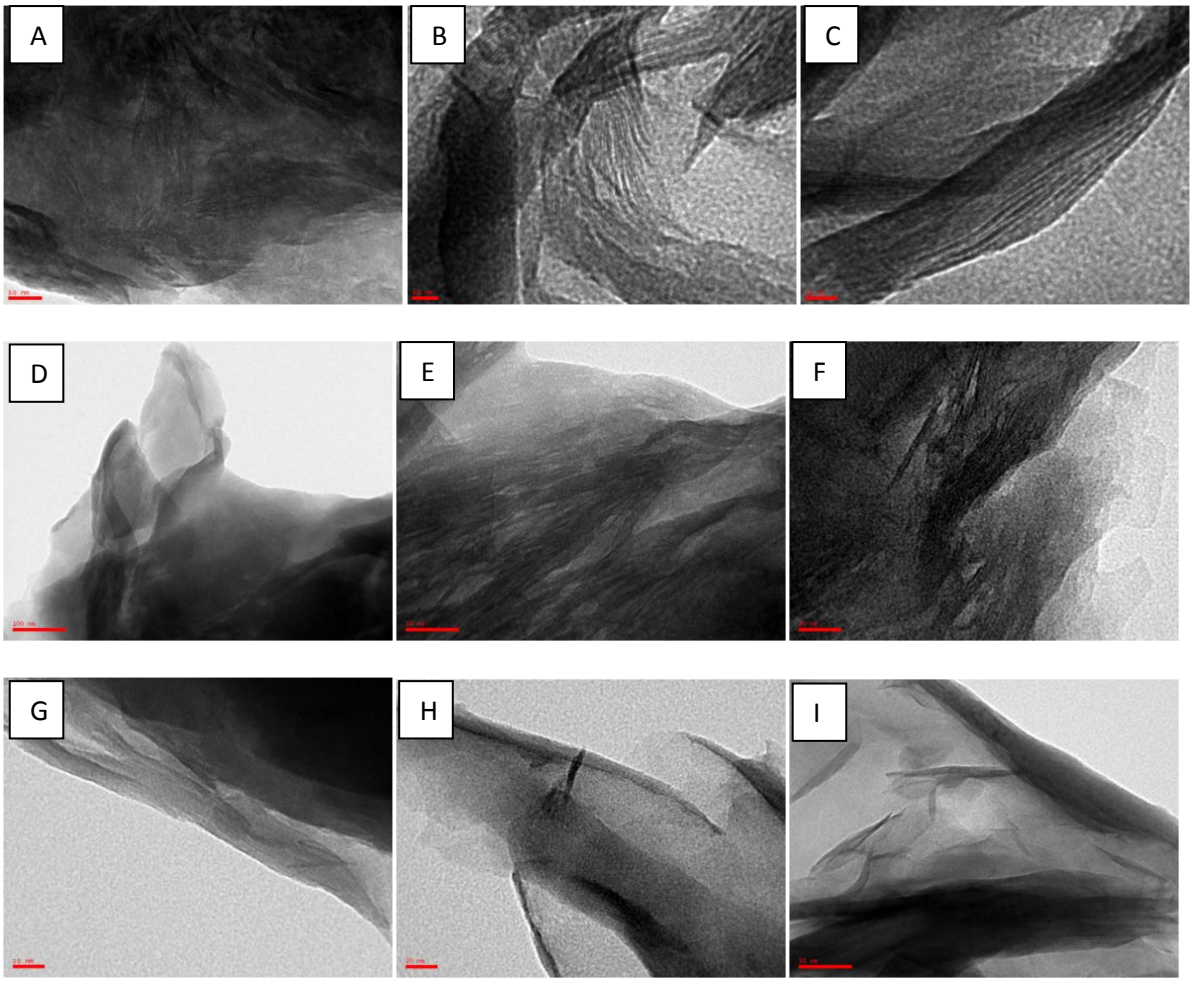

Figure 29. TEM images of CG-MMT 3:1 (A), (B) and (C). Scale bar represents 50 nm (A), 10 nm (B), 10 nm (C). TEM images of NG-MMT 3:1 (D), (E) and (F). Scale bar represents 100 nm (D), 50 nm (E), 20nm (F). TEM images of NG-MMT 6:1 (G), (H) and (I). Scale bar represents 20 nm (G), 20nm (H) and 50 nm (I).

Figure 30 shows the TG trace of CG-MMT 3:1 and Figure 31 shows the DTG trace of CG-MMT 3:1, in comparison to Na^+ MMT. Two steps are distinctly observed in the case of Na^+ MMT. First, montmorillonite undergoes desorption of the water within the temperature range of 25 ºC - 100 ºC corresponding to a weight loss of approximately 5%. This stage is followed by dehydroxylation, with the subsequent loss of the chemically absorbed water within the temperature range of 560 ºC – 700 ºC (Hoidy *et al.*, 2009; Xie *et al*., 2001; Fajnor & Jesenák, 1996; Girgis *et al*., 1987*).*

The DTG trace of CG-MMT 3:1 reveals the loss of water as a broad peak centered at 63 ℃. The loss of the cationic guar constituent of the nanocomposite is indicated as a broad peak centered at 280 ℃ with a small shoulder centered at 342 ℃. In comparison, the thermal decomposition of cationic guar gum (Fig. 32) appears as a single sharp peak on the DTG trace centered at 287 ℃. The broadness of the DTG peak and the existence of a shoulder can be interpreted as the effect of polymer interaction with the clay. The total weight loss of CG-MMT 3:1 is 47.6% while the total weight loss of Na^+ MMT is 9.63%, further signifying the uptake of the cationic guar gum. Although the adsorption process occurs through a desorption of water molecules (Gu & Done, 1992), the TGA trace of the nanocomposite reveals a greater content of physically adsorbed water, in comparison to starting montmorillonite which can be interpreted as due to the hydration of residual cationic guar gum, adsorbed onto surface regions of montmorillonite.

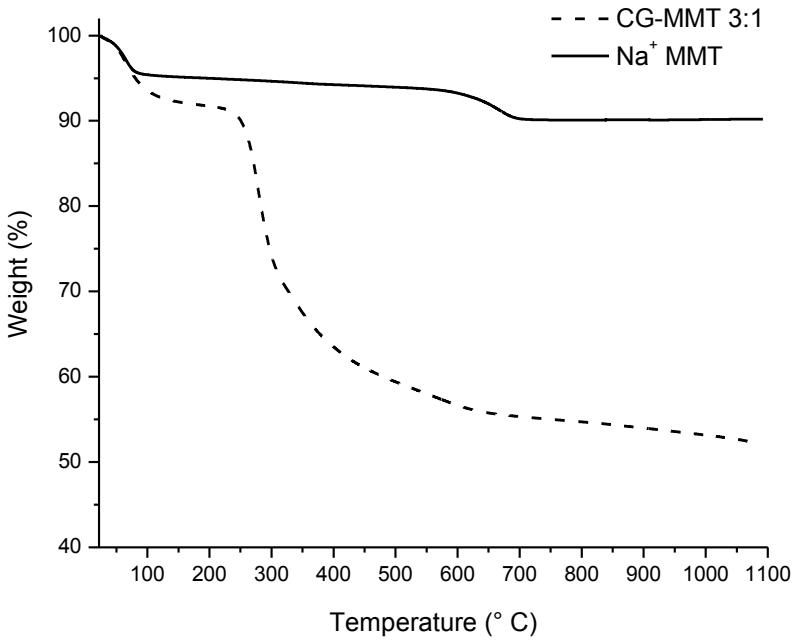

Figure 30. TG traces of Na^+ MMT and CG-MMT 3:1.

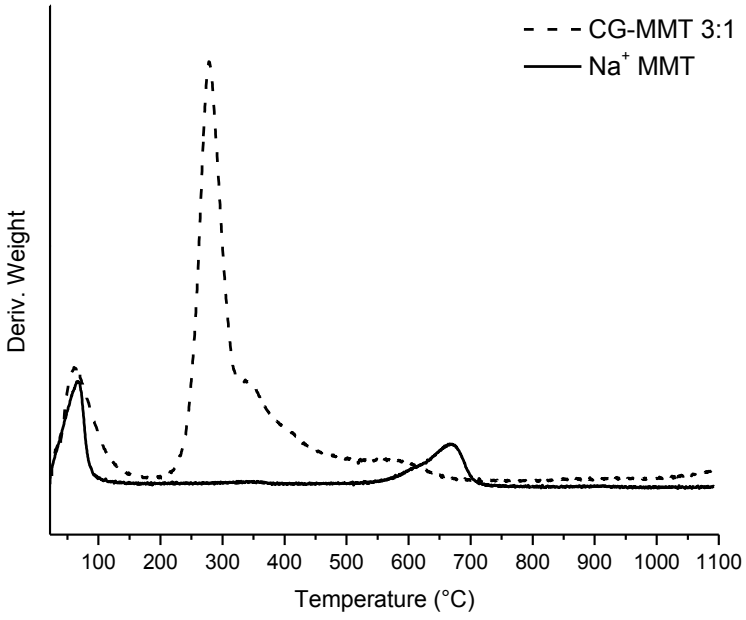

Figure 31. DTG traces of Na^+ MMT and CG-MMT 3:1.

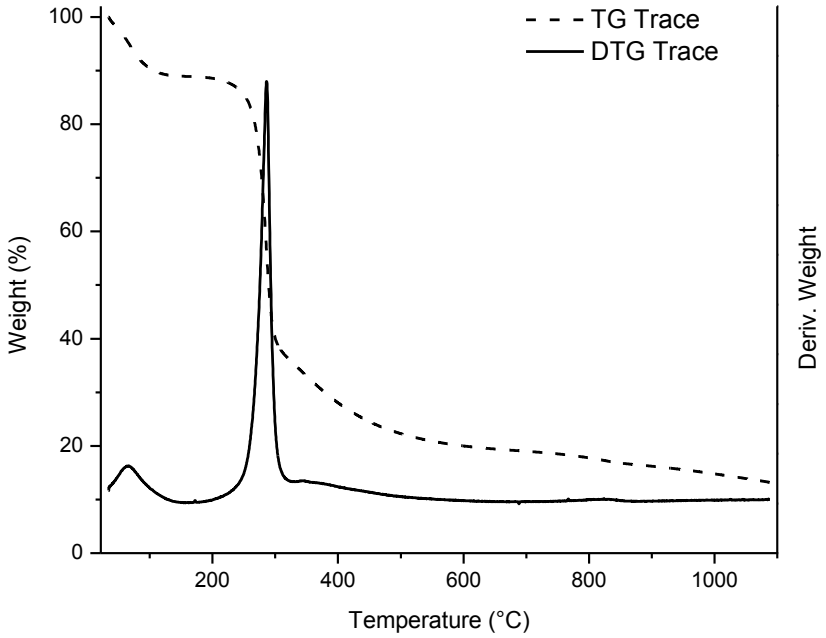

Figure 32. TG and DTG traces of cationic guar gum.

Figure 33 shows the TG traces of NG-MMT 3:1 and NG-MMT 6:1, in comparison to Na^+ MMT. Figure 34 shows the DTG traces of NG-MMT 3:1 and NG-MMT 6:1, in comparison to Na^+ MMT. The DTG traces of NG-MMT 3:1 and NG-MMT 6:1 reveal the loss of water as broad peaks, both centered at approximately 70℃. Also, in both cases, the loss of the neutral guar constituent of the nanocomposite occurs in multiple steps and over a broad temperature range. The DTG trace of NG-MMT 3:1 indicates the loss of neutral guar by 2 peaks centered at 253℃ and 304℃, and a shoulder centered at approximately 347℃. The DTG trace of NG-MMT 6:1 indicates the loss of neutral guar by 3 peaks centered at 261℃, 309℃ and 350℃. In comparison, the thermal decomposition of neutral guar gum (Fig. 35) appears as a single sharp peak on the DTG trace centered at 305℃. If the adsorption of cationic guar gum is analogous to that of alkylammonium, then the loss of

organic in multiple steps indicates varying thermal stabilities (Langier-Kuzniarowa, 2002). As a constituent of the nanocomposite, neutral guar gum can be surface adsorbed or intercalated within the interlamellar space as part of a monolayer or bilayer, and these varying environments result in a range of thermal stabilities. Likewise, the TGA traces of NG-MMT 3:1 and NG-MMT 6:1 (Fig. 33), reveal total weight losses of 51.7% and 55.8% respectively, corresponding to the decomposition of the neutral guar gum, confirming the adsorption.

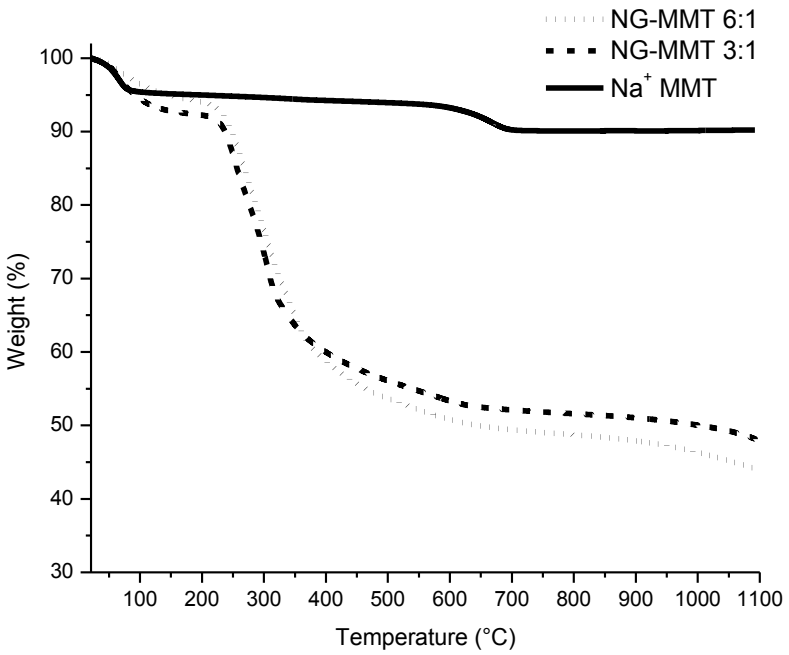

Figure 33. TG traces of Na^+ MMT, NG-MMT 3:1 and NG-MMT 6:1

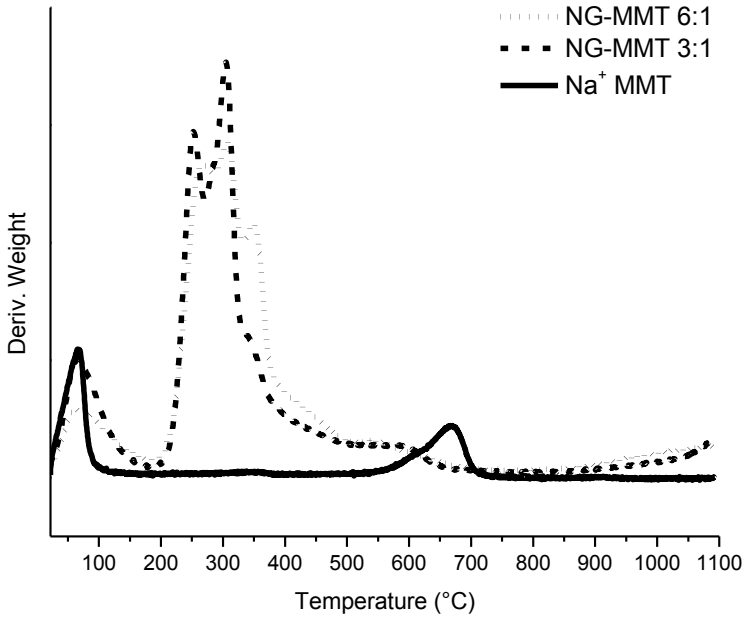

Figure 34. DTG traces of Na^+ MMT, NG-MMT 3:1, NG-MMT 6:1

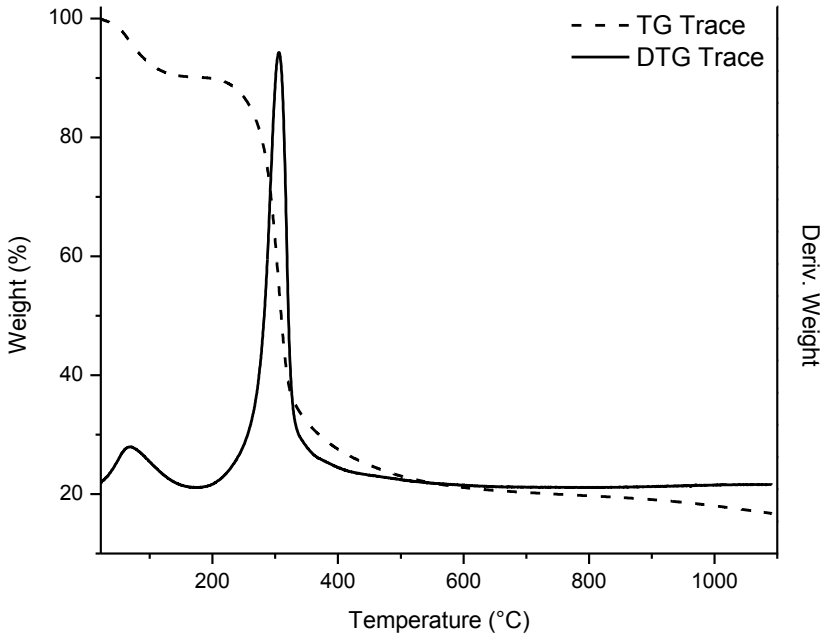

Figure 35. TG and DTG traces of neutral guar gum.

Although the supplier of neutral guar gum (Sigma-Aldrich) provided a total ash content of ≤1 %, as indicated by the product specifications, this may not be the case since the TG trace of neutral guar gum (Fig. 35) indicates that 16.7% of the sample is left remaining at a temperature of 1100℃. As well, the TG trace of cationic guar gum (Fig. 32) indicates that 13.5% of the sample is left remaining at 1100℃.

The ^{13}C CP-MAS NMR spectrum of CG-MMT (Fig. 36) reveals signals corresponding to cationic guar gum, thereby confirming the uptake. The ^{13}C CP-MAS spectrum of NG-MMT 3:1 (Fig. 37) also reveals signals corresponding to neutral guar gum confirming the uptake, as well as the presence of other unexpected minor peaks. Two peaks in the range of 170.0 ppm and 174.5 ppm, seen in the ^{13}C CP-MAS NMR spectrum of

NG-MMT 3:1 and a broader peak centered at 173.0 ppm, seen in the ^{13}C CP-MAS NMR spectrum of NG-MMT 6:1, indicate the existence of carboxyl carbons, which appear to be absent in the NMR spectrum of neutral guar gum (NG) (Fig. 37).

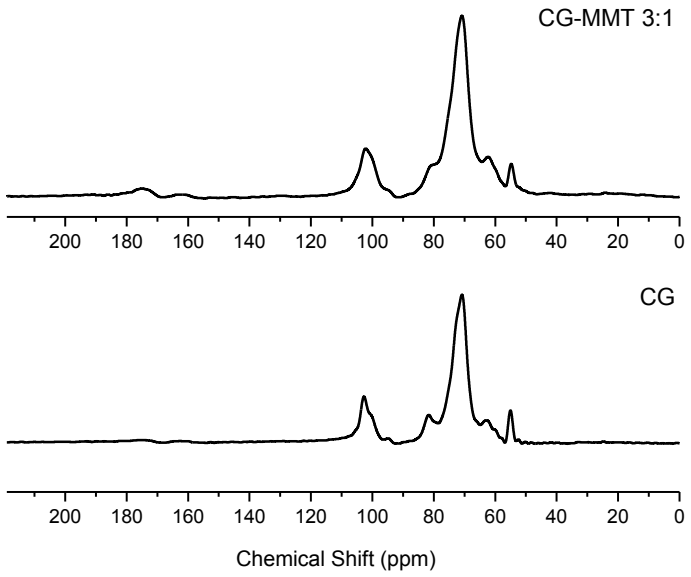

Figure 36. ^{13}C CP-MAS NMR of CG and CG-MMT 3:1.

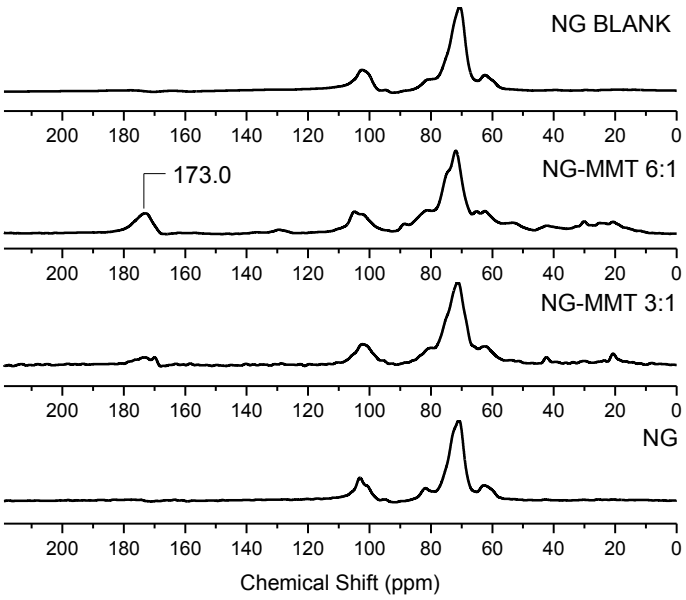

Figure 37. ^{13}C CP-MAS NMR of NG, NG-MMT 3:1, NG-MMT 6:1 and NG BLANK.

To further investigate the appearance of the carboxyl carbon peaks in the NMR spectrum, a blank experiment was performed with neutral guar gum in the absence of montmorillonite. The ^{13}C CP-MAS NMR spectrum of the blank experiment (NG BLANK) (Fig. 37) is very similar to starting neutral guar gum (NG), with an absence of peaks in the carboxyl carbon region. The absence of carboxyl carbon peaks in the spectrum of NG BLANK indicates that the existence of montmorillonite is a causative factor for their appearance. The findings of Tiraferri *et al.* (2008) indicate carboxyl functional groups on guar gum molecules, as impurities in commercial guar gum. For this reason, the presence of the carboxyl carbon peaks in the NMR spectrum of the nanocomposites, and their absence in the spectrum of NG BLANK may occur due to a preferential accumulation of guar molecules containing the carboxyl functional groups by montmorillonite, resulting in an observable peak in the NMR spectrum.

In addition, one cannot exclude the possibility of a catalytic role played by montmorillonite as a causative factor for the presence of carboxyl carbons. Clay minerals, in particular smectites, are known to catalyze a number of organic reactions (Adams & McCabe, 2006). However, to the best of my knowledge, there is not yet any evidence of montmorillonite reacting with polysaccharides to catalyze the formation of carboxylic acids.

^{23}Na NMR spectrum of CG-MMT 3:1 (Fig. 38) reveals the absence of sodium cations. This is expected since the intercalation of cationic compounds occurs through the conventional cation exchange method, where the sodium cations in the interlamellar space of Na^+ MMT are exchanged for cationic guest molecules. On the other hand, ^{23}Na NMR spectra of NG-MMT 3:1 and NG-MMT 6:1 (Fig. 38) also indicate an absence of signal. The reason for this may be attributed to the presence of cationic impurities in guar gum. According to product specifications provided by the supplier (Sigma-Aldrich), an ash impurity is present and according to literature, impurities such as potassium, calcium, sodium and iron are associated with guar gum (Debon & Tester, 2001). These cations can replace the exchangeable cations of the interlayer space of montmorillonite. Indeed the ICP-MS results (Table 2) indicate an increase in the potassium and calcium content, and a decrease in sodium content of the nanocomposites (NG-MMT 3:1 and NG-MMT 6:1), as opposed to starting Na^+ MMT; this verifies that during the preparation of the nanocomposite, potassium and calcium cations exchanged with the sodium cations of the interlayer space of montmorillonite. Also, the aluminum, magnesium and iron concentrations of the nanocomposites and Na^+ MMT were compared (Table 2). By taking into account the structural aluminum, magnesium and iron contributions to the ICP-MS-determined concentrations, it is revealed that the concentrations of these ions do not vary significantly in

Na^+ MMT and the nanocomposites. Since sodium, potassium and calcium account for less than 40% of the CEC of Na^+ MMT (74.5 meq/100g of clay), additional inorganic ions, that were not tested for, must be present in the sample.

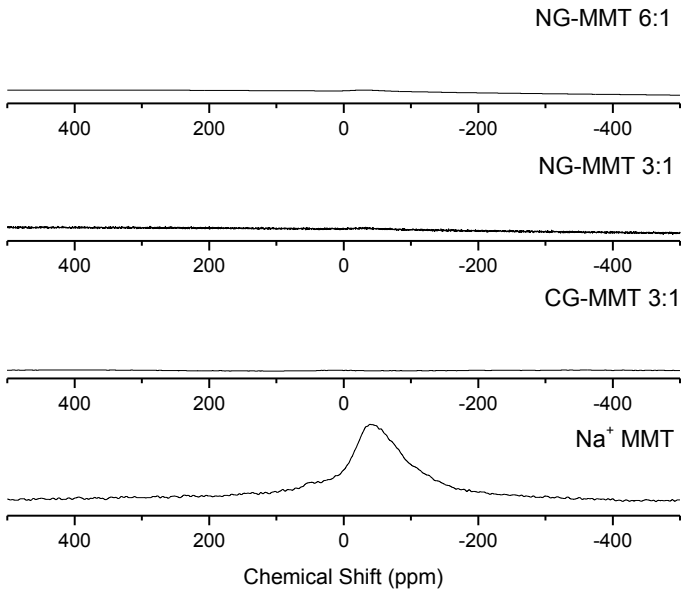

Figure 38. ^{23}Na NMR of Na^+ MMT, CG-MMT 3:1, NG-MMT 3:1 and NG-MMT 6:1.

Concentration (ppm)	**Al**	**Ca**	**Fe**	**K**	**Mg**	**Na**
NG-MMT 3:1	4397	985	1442	2170	1174	4241
NG-MMT 6:1	3159	1418	1221	2355	1236	2767
Na^+ MMT	6576	339	2514	201	1340	16625

Table 2. ICP-MS determined concentrations of various cations present in Na^+ MMT, NG-MMT 3:1, NG-MMT 6:1, as determined by ICP-MS.

Nanocomposites are known to be diverse materials with a multitude of applications in many avenues. Polymer/ layered silicate nanocomposites often exhibit a significant improvement in properties, generating interest and finding applications in many facets of academia and industry (Hule & Pochan, 2007; Suresh *et al.*, 2010). Bionanocomposites, synthesized using a biodegradable compound such as guar gum, are especially advantageous for use in the pharmaceutical industry (Hule & Pochan, 2007). The pharmaceutical applications of clay minerals are well known and many of these uses employ the adsorptive capacity of clay minerals for organic compounds (Aguzzi *et al.*, 2007). Compared with unmodified montmorillonite, guar-montmorillonite should possess a greater capacity for the accommodation of neutral organic molecules, due to the enhancement of the interlayer space as well as improved organophilicity (An & Dultz, 2007; Suresh *et al.*, 2010; Wang *et al.*, 2008). If the uptake of cations exceeds the cation exchange capacity, an adsorptive capacity for anions is generated (An & Dultz, 2007). Generally, the capacity of unmodified clays to adsorb anions is low, with the adsorption occurring only on the edges of the aluminosilicate layers. In the case of CG-MMT 3:1, when an excess of cationic guar gum is intercalated,

chloride anions may become associated with the clay in order to achieve electric neutrality. This provides a potentiality for the uptake of anionic drugs, though an anion exchange with chloride. If the behaviour of a cationic polysaccharide, such as cationic guar gum, is analogous to that of other polycations, localities of excess positive charge on the clay may develop due to loops and trains formed by the adsorbed polysaccharide. These positive patches provide segments capable of anion adsorption (Churchman *et al.*, 2006).

4. 5 Conclusion

Two novel nanocomposites were successfully prepared and characterized. With cationic guar gum, the CG-MMT 3:1 nanocomposite was prepared and characterized as possessing an intercalated morphology, with a monolayer orientation of the cationic guar gum within the interlayer space. With neutral guar gum, the NG-MMT nanocomposites exhibit a mixed morphology with intercalated regions and delaminated regions. NG-MMT 3:1 was characterized as possessing both monolayer orientations and bilayer orientations of neutral guar gum in the interlamellar space. When using a higher neutral guar gum content during the preparation process, the resultant NG-MMT 6:1 nanocomposite revealed a predominant formation of the bilayer and delamination. Since these novel nanocomposites are composed of a biodegradable polymer, potential applications in the pharmaceutical field are especially attractive. The improvement of the organophilicity of the clay minerals and the enhancement of the interlayer space can attribute adsorptive capabilities to the nanocomposite, signifying its potential use as a drug carrier (Suresh *et al.*, 2010).

References

Adams, J. M. & McCabe, R. W. (2006). Clay Minerals as Catalysts. In F. Bergaya, B. K. G. Theng & G. Lagaly (Eds.), *Handbook of Clay Science* (pp. 541-581). Amsterdam: Elsevier.

Aguzzi, C., Cerezo, P., Viseras, C., & Caramella, C. (2007). Uses of clays as drug delivery systems: Possibilities and limitations. *Applied Clay Science, 36*(1-3), 22-36.

Ahmadi, S. J., Huang, Y. D., & Li, W. S. (2004). Synthetic routes, properties and future applications of polymer-layered silicate nanocomposites. *Journal of Materials Science, 39*(6), 1919-1925.

An, J. H., & Dultz, S. (2007). Polycation adsorption on montmorillonite: pH and T as decisive factors for the kinetics and mode of chitosan adsorption. *Clay Minerals, 42*(3), 329-339.

Bhiwankar, N. N., & Weiss, R. A. (2006). Melt intercalation/exfoliation of polystyrene-sodium-montmorillonite nanocomposites using sulfonated polystyrene ionomer compatibilizers. *Polymer, 47*(19), 6684-6691.

Campbell, K., Craig, D. Q. M., & McNallya, T. (2008). Poly(ethylene glycol) layered silicate nanocomposites for retarded drug release prepared by holt-melt extrusion. *International Journal of Pharmaceutics, 363*(1-2), 126-131.

Carrado, K. A., Decarreau, A., Petit, S., Bergaya, F., & Lagaly, G. (2006). Synthetic clay minerals and purification of natural clays. In F. Bergaya, B. K. G. Theng & G. Lagaly (Eds.), *Handbook of Clay Science* (pp.115-139). Amsterdam: Elsevier.

Choudalakis, G., & Gotsis, A. D. (2009). Permeability of polymer/clay nanocomposites: A

Review. *European Polymer Journal, 45*(4), 967-984.

Chudzikowski, R. J. (1971). Guar gum and its applications. *Journal of the Society of Cosmetic Chemists, 22*, 43-60.

Churchman, G. J., Gates, W. P., Theng, B. K. G., & Yuan, G. (2006). Clays and clay minerals for pollution control. In F. Bergaya, B. K. G. Theng & G. Lagaly (Eds.), *Handbook of Clay Science* (pp. 625-675). Amsterdam: Elsevier.

Cypes, S. H., Saltzman, W. M., & Giannelis, E. P. (2003). Organosilicate-polymer drug delivery systems: Controlled release and enhanced mechanical properties. *Journal of Controlled Release, 90*(2), 163-169.

Darder, M., Colilla, M., & Ruiz-Hitzky, E. (2003). Biopolymer−Clay Nanocomposites based on Chitosan Intercalated in Montmorillonite. *Chemistry of Materials, 15* (20), pp 3774–3780.

De Souza, C. E. C., Lima, A. S., & Nascimento, R. S. V. (2010). Hydrophobically modified poly(ethylene glycol) as reactive clays inhibitor additive in water-based drilling fluids. *Journal of Applied Polymer Science, 117*(2), 857-864.

Debon, S. J. J., & Tester, R. F. (2001). In vitro binding of calcium, iron and zinc by non-starch polysaccharides. *Food Chemistry, 73*(4), 401-410.

Fajnor, V. S., & Jesenák, K. (1996). Differential thermal analysis of montmorillonite. *Journal of Thermal Analysis, 46*(2), 489-493.

Girgis, B. S., El-Baraway, K. A., & Felix, N. S. (1987). Dehdyration kinetics of some smectites: A thermogravimetric study. *Thermochimica Acta, 111*, 9-19.

Gliko-Kabir, I., Penhasi, A., & Rubinstein, A. (1999). Characterization of crosslinked guar by thermal analysis. *Carbohydrate Research, 316*(1-4), 6-13.

Gu, B., & Done, H. E. (1992). The interaction of polysaccharides with silver hill illite. *Clays and Clay Minerals, 40*(2), 151-156.

Hoidy, W. H., Mansor, B., Ahmad, E. A., Jaffar, A. M., & Nor, A. B. I. (2009). Synthesis and characterization of organoclay from sodium montmorillonite and fatty hydroxamic acids. *American Journal of Applied Sciences, 6*(8), 1567-1572.

Hule, R. A., & Pochan, D. J. (2007). Polymer nanocomposites for biomedical applications. *MRS Bulletin, 32*(4), 354-358.

Iqbal, M. (1993). International trade in non-wood forest products: an overview. *Food and Agriculture Organization of the United Nations, Rome.* Retrieved January 30, 2011, from http://www.fao.org/docrep/x5326e/x5326e08.htm

Kaplan, D. L. (1998). Introduction to biopolymers from renewable resources. In D. L. Kapla (Ed.), *Biopolymers from renewable resources* (pp. 1-26). Berlin: Springer.

Kreer, M., Swami, G., Kumar, R., Kanwar, K., Kaur, P., Singh, P., & Kaur, A. (2010). Applications of novel excipients in the allopathic and herbal formulations. *Journal of Chemical and Pharmaceutical Research, 2*(4), 851-860.

Langier-Kuzniarowa, A. (2002). Thermal analysis of organo-clay complexes. In S. Yariv, & H. Cross (Eds.), *Organo-clay complexes and interactions* (1st ed., pp. 273-344). New York: Marcel Dekker.

Lapasin, R., & Pricl, S. (1999). *Rheology of industrial polysaccharides: Theory and Applications.* Gaithersburg, MD: Aspen Publications.

Lee, W. F., & Fu, Y. T. (2003). Effect of montmorillonite on the swelling behavior and drug-release behavior of nanocomposite hydrogels. *Journal of Applied Polymer Science, 89*(13), 3652-3660.

Levy, N., Garti, N., & Magdassi, S. (1995). Flocculation of bentonite suspensions with cationic guar. *Colloids and Surfaces A: Physicochemical and Engineering Aspects, 97*(2), 91-99.

Martín, Z., Jiménez, I., Gómez, M. A., Ade, H. W., Kilcoyne, D. A., & Hernádez-Cruz, D. (2009). Spectromicroscopy study of intercalation and exfoliation in Propylene/Montmorillonite nanocomposites. *The Journal of Physical Chemistry B, 113*(32), 11160-11165.

Okamoto, M. (2005). Biodegradable Polymer/Layered silicate nanocomposites: A review. In S. Mallapragada, & B. Narasimhan (Eds.), *Handbook of Biodegradable Polymeric Materials and their Applications* (pp. 1-45). Stevenson Ranch, CA: American Scientific Publishers.

Oriakhi, C. O. (2000). Polymer nanocomposition approach to advanced materials. *Journal of Chemical Education, 77*(9), 1138-1146.

Park, H. M., Misra, M., Drzal, L. T., & Mohant, A. K. (2004). "Green" nanocomposites from cellulose acetate bioplastic and clay: Effect of eco-friendly triethyl citrate plasticizier. *Biomacromolecules, 56*(6), 2281-2288.

Ray, S. S., & Okamoto, M. (2003). Polymer/layered silicate nanocomposites: A review from preparation to processing. *Progress in Polymer Science, 28*(11), 1539-1641.

Ray, S. S., & Bousmina, M. (2005). Biodegradable polymers and their layered silicate nanocomposites: In greening the 21st century materials world. *Progress in Materials Science, 50*(8), 962-1079.

Ray, S. S., Okamoto, K., & Okamoto, M. (2003). Structure-Property relationship in

biodegradable poly(butylene succinate)/Layered silicate nanocomposites. *Macromolecules, 36*(7), 2355-2367.

Rhim, J. W., & Ng, P. K. (2007). Natural biopolymer-based nanocomposite films for packaging applications. *Critical Reviews in Food Science and Nutrition*, *47*(4), 411-433.

Ruiz-Hitzky, E., & van Meerbeek, A. (2006). Clay mineral-and organoclay- polymer nanocomposite. In F. Bergaya, B. K. G. Theng, & G. Lagaly (Eds.), *Handbook of Clay Science* (pp. 583-621). Amsterdam: Elsevier.

Ruiz-Hitzky, E., Darder, M., & Aranda, P. (2005). Functional biopolymer nanocomposites based on layered solids. *Journal of Materials Chemistry, 15*(35-36), 3650-3662.

Srivastava, M., & Kapoor, V. P. (2005). Seed galactomannans: An overview. *Chemistry Biodiversity, 2*(3), 295-317.

Suresh, R., Borkar, S. N., Sawant, V. A., Shende, V. S., & Dimble, S. K. (2010). Nanoclay drug delivery system. *International Journal of Pharmaceutical Sciences and Nanotechnology, 3*(2). 901-905.

Theng, B. K. G. (1979). *Formation and properties of clay-polymer complexes.* Amsterdam: Elsevier.

Tiraferri, A., Chen, K. L., Sethi, R., & Elimelech, M. (2008). Reduced aggregation and sedimentation of zero-valent iron nanoparticles in the presence of guar gum. *Journal of Colloid and Interface Science*, *324*(1-2), 71-79.

Verbeken, D., Dierckx, S., & Dewettinck, K. (2003). Exudate gums: Occurrence, production, and applications. *Applied Microbiology and Biotechnology, 63*(1), 10-21.

Wang, X., Du, Y., & Luo, J. (2008). Biopolymer/montmorillonite nanocomposite:

Preparation, drug-controlled release property and cytotoxicity. *Nanotechnology,* 19(6), 1-7.

Wegner, T. H., & Jones, E. P. (2009). A fundamental review of the relationships between nanotechnology and lignocellulosic biomass. In L. Lucia, & O. Rojas (Eds.), *The Nanoscience and Technology of Renewable Biomaterials* (pp. 1-38). West Sussex, UK: Wiley.

Xie, W., Gao, Z., Pan, W., Huner, D., Singh, A., & Vaia, R. (2001). Thermal degradation chemistry of alkyl quaternary ammonium montmorillonite. *Chemistry of Materials, 13*(9), 2979-2990.

General Conclusions

The clay mineral montmorillonite possesses a large surface area, good adsorbability, a cation exchange capacity, as well as an inert toxicity. These properties allow montmorillonite to be used as an ingredient in many pharmaceutical products. The use of montmorillonite is significantly broadened by modulation of its properties. In the case of an alkylammonium-montmorillonite, such modifications enabled for the intercalation of oxybenzone, as indicated by thermal analysis and ^{13}C NMR results. Future work would involve investigating the adsorption of oxybenzone using montmorillonite modified with different organic cations, in order to optimize the adsorption. The use of montmorillonite alongside UV filters is very attractive in the sense that this would involve the incorporation of a naturally occurring, abundant and inexpensive material in order to address limitations of conventional UV filters.

Polymer nanocomposites are highly sought after due to their applicability in a variety of avenues, making this a very active area of research. Novel nanocomposites were synthesised using cationic guar gum and neutral guar gum. XRD and TEM have shown that intercalated structures can be produced in both cases. The cationic guar-montmorillonite nanocomposite exhibits a monolayer orientation of the cationic guar within the interlayer space. On the other hand, neutral guar nanocomposites reveal both monolayer and bilayer orientations of neutral guar within the interlayer space. TEM allowed for the observance of the delaminated regions of the neutral guar-montmorillonite nanocomposites, which are XRD-silent. Pre- modification of montmorillonite was not required to synthesize these nanocomposites, and this is very attractive for industrial use from an economic perspective.

Moreover, the synthesis of the nanocomposites was performed by adhering to principles of green chemistry which include the incorporation of biodegradable and nontoxic materials, and the lack of solvent or toxic chemical use. The incorporation of a biopolymer as the organic constituent makes these nanocomposites attractive for medical applications. Also, it was shown that the preparation of these nanocomposites using different ratios of polymer:clay led to differing morphologies, and so further work could involve optimizing the levels of clay and polymer to achieve the desired structure.